Earth Syst. Sci. Data, 15, 2695–2710, 2023
https://doi.org/10.5194/essd-15-2695-2023

Open Access Earth System Science Data

Antarctic Bedmap data: Findable, Accessible, Interoperable, and Reusable (FAIR) sharing of 60 years of ice bed, surface, and thickness data

Alice C. Frémand[1,★], Peter Fretwell[1,★], Julien A. Bodart[2,1,★], Hamish D. Pritchard[1], Alan Aitken[3], Jonathan L. Bamber[4,49], Robin Bell[5], Cesidio Bianchi[6], Robert G. Bingham[2], Donald D. Blankenship[7], Gino Casassa[8,56], Ginny Catania[7], Knut Christianson[9], Howard Conway[9], Hugh F. J. Corr[1], Xiangbin Cui[10], Detlef Damaske[11], Volkmar Damm[11], Reinhard Drews[12], Graeme Eagles[13], Olaf Eisen[13,50], Hannes Eisermann[13], Fausto Ferraccioli[14,1], Elena Field[1], René Forsberg[15], Steven Franke[13], Shuji Fujita[16], Yonggyu Gim[17], Vikram Goel[18], Siva Prasad Gogineni[19], Jamin Greenbaum[20,7], Benjamin Hills[21], Richard C. A. Hindmarsh[1,✝], Andrew O. Hoffman[5], Per Holmlund[22], Nicholas Holschuh[23], John W. Holt[24], Annika N. Horlings[9], Angelika Humbert[13,50], Robert W. Jacobel[25], Daniela Jansen[13], Adrian Jenkins[26], Wilfried Jokat[13,50], Tom Jordan[1], Edward King[1], Jack Kohler[27], William Krabill[28], Mette Kusk Gillespie[41], Kirsty Langley[29], Joohan Lee[30], German Leitchenkov[31], Carlton Leuschen[32], Bruce Luyendyk[33], Joseph MacGregor[34], Emma MacKie[35,51], Kenichi Matsuoka[36], Mathieu Morlighem[37], Jérémie Mouginot[38,52,✝], Frank O. Nitsche[5], Yoshifumi Nogi[16], Ole A. Nost[36], John Paden[32], Frank Pattyn[39], Sergey V. Popov[40], Eric Rignot[38,53,17], David M. Rippin[42], Andrés Rivera[43], Jason Roberts[44,54], Neil Ross[45], Anotonia Ruppel[11], Dustin M. Schroeder[35,55], Martin J. Siegert[46], Andrew M. Smith[1], Daniel Steinhage[13], Michael Studinger[47], Bo Sun[10], Ignazio Tabacco[6,✝], Kirsty Tinto[5], Stefano Urbini[6], David Vaughan[1,✝], Brian C. Welch[25], Douglas S. Wilson[48], Duncan A. Young[7], and Achille Zirizzotti[6]

[1]British Antarctic Survey, Cambridge, UK
[2]School of GeoSciences, University of Edinburgh, Edinburgh, UK
[3]School of Earth Sciences, The University of Western Australia, Perth, Australia
[4]School of Geographical Sciences, University of Bristol, Bristol, UK
[5]Lamont-Doherty Earth Observatory, Columbia University, Palisades, USA
[6]Istituto Nazionale di Geofisica e Vulcanologia, Rome, Italy
[7]Institute for Geophysics, University of Texas at Austin, Austin, USA
[8]General Directorate of Water (DGA), Santiago, Chile
[9]Earth and Space Sciences, University of Washington, Seattle, USA
[10]Polar Research Institute of China, Shanghai, China
[11]Bundesanstalt für Geowissenschaften und Rohstoffe, Hanover, Germany
[12]Department of Geosciences, Tübingen University, Tübingen, Germany
[13]Alfred Wegener Institute, Helmholtz Centre for Polar and Marine Research, Bremerhaven, Germany
[14]Istituto Nazionale di Oceanografia e di Geofisica Sperimentale, Trieste, Italy
[15]DTU Space, Lyngby, Denmark
[16]National Institute of Polar Research, Tokyo, Japan
[17]Jet Propulsion Laboratory, California Institute of Technology, Pasadena, USA
[18]National Centre for Polar & Ocean Research (NCPOR), Ministry of Earth Sciences, Vasco-da Gama, Goa – 403804, India
[19]University of Alabama, Tuscaloosa, AL 35487, USA
[20]Scripps Institution of Oceanography, La Jolla, USA
[21]Department of Earth and Space Sciences, University of Washington, Seattle, USA
[22]Stockholm University, Stockholm, Sweden

Published by Copernicus Publications.

[23]Amherst College, Amherst, USA
[24]University of Arizona, Tucson, USA
[25]St. Olaf College, Northfield, MN 55057, USA
[26]Northumbria University, Newcastle, UK
[27]Norwegian Polar Institute, Fram Centre, Tromsø, Norway
[28]NASA Wallops Flight Facility, Wattsville, VA, USA
[29]Asiaq, Greenland Survey, Nuuk, Greenland
[30]Korean Polar Research Institute, Incheon, South Korea
[31]Institute for Geology and Mineral Resources of the World Ocean, St. Petersburg, Russia
[32]Centre for Remote Sensing of Ice Sheets, University of Kansas, Lawrence, USA
[33]Earth Research Institute, University of California in Santa Barbara, USA
[34]Cryospheric Sciences Lab, NASA Goddard Space Flight Center, Greenbelt, MD, USA
[35]Department of Geophysics, Stanford University, Stanford, CA, USA
[36]Oceanbox.io, Tromsø, Norway
[37]Department of Earth Sciences, Dartmouth College, Hanover, USA
[38]Department of Earth System Science, University of California Irvine, Irvine, CA, USA
[39]Laboratoire de Glaciologie, Université Libre de Bruxelles, Brussels, Belgium
[40]Polar Marine Geosurvey Expedition, St. Petersburg, Russia
[41]Western Norway University of Applied Sciences, Bergen, Norway
[42]Department of Environment and Geography, University of York, York, UK
[43]Departamento de Geografía, Universidad de Chile, Santiago, Chile
[44]Australian Antarctic Program Partnership, Institute for Marine & Antarctic Studies, University of Tasmania, Hobart, Australia
[45]School of Geography, Politics and Sociology, Newcastle University, Newcastle-upon-Tyne, UK
[46]Grantham Institute and Department of Earth Science and Engineering, Imperial College London, London, UK
[47]NASA Goddard Space Flight Center, Greenbelt, USA
[48]Marine Science Institute, University of California, Santa Barbara, USA
[49]Department of Aerospace and Geodesy, Technical University of Munich, Munich, Germany
[50]Department of Geoscience, University of Bremen, Bremen, Germany
[51]Department of Geological Sciences, University of Florida, Gainesville, USA
[52]University of Grenoble Alpes, CNRS, IRD, Grenoble INP, IGE, Grenoble, France
[53]Department of Civil and Environmental Engineering, University of California Irvine, Irvine, CA, USA
[54]Australian Antarctic Division, Kingston, Australia
[55]Department of Electrical Engineering, Stanford University, Stanford, CA, USA
[56]University of Magallanes, Punta Arenas, Chile
★These authors contributed equally to this work.
†deceased

Correspondence: Alice C. Frémand (almand@bas.ac.uk) and Peter Fretwell (ptf@bas.ac.uk)

Received: 19 October 2022 – Discussion started: 22 November 2022
Revised: 31 March 2023 – Accepted: 9 April 2023 – Published: 17 July 2023

Abstract. One of the key components of this research has been the mapping of Antarctic bed topography and ice thickness parameters that are crucial for modelling ice flow and hence for predicting future ice loss and the ensuing sea level rise. Supported by the Scientific Committee on Antarctic Research (SCAR), the Bedmap3 Action Group aims not only to produce new gridded maps of ice thickness and bed topography for the international scientific community, but also to standardize and make available all the geophysical survey data points used in producing the Bedmap gridded products. Here, we document the survey data used in the latest iteration, Bedmap3, incorporating and adding to all of the datasets previously used for Bedmap1 and Bedmap2, including ice bed, surface and thickness point data from all Antarctic geophysical campaigns since the 1950s. More specifically, we describe the processes used to standardize and make these and future surveys and gridded datasets accessible under the Findable, Accessible, Interoperable, and Reusable (FAIR) data principles. With the goals of making the gridding process reproducible and allowing scientists to re-use the data freely for their own analysis, we introduce the new SCAR Bedmap Data Portal (https://bedmap.scar.org, last access: 1 March 2023) created to provide unprecedented open access to these important datasets through a web-map interface. We believe that

this data release will be a valuable asset to Antarctic research and will greatly extend the life cycle of the data held within it. Data are available from the UK Polar Data Centre: https://data.bas.ac.uk (last access: 5 May 2023). See the Data availability section for the complete list of datasets.

1 Introduction

Detailed and extensive information on ice thickness and bed topography is needed to reconstruct the geological and geomorphic history of Antarctica and to model ice flow in order to predict the ice sheet's future contribution to sea level rise (Fretwell et al., 2013; DeConto and Pollard, 2016; Scambos et al., 2017; The IMBIE team, 2018; Rignot et al., 2019; Morlighem et al., 2020; DeConto et al., 2021; Fox-Kemper et al., 2021). This information has primarily been gathered using ground-based or airborne radio-echo sounding (RES) and seismic surveys conducted by over 50 institutions under multiple national programmes across Antarctica over the last 60 years. However, up until now, these survey datasets have not been held centrally or been standardized, thus limiting their accessibility to the wider Antarctic community. Consequently, previous attempts to map the ice sheet on the continental scale, such as Bedmap1 (Lythe and Vaughan, 2001), Bedmap2 (Fretwell et al., 2013) and Bedmachine Antarctica (Morlighem et al., 2020), have had to first find data, gain permissions, and download, clean and standardize hundreds of datasets from survey campaigns of many different sources before finally constructing the grids. These constraints have led to only a limited number of gridded products being made, often years apart and with a long lag after the surveys have been completed. Given the rapidity of change affecting large parts of the Antarctic Peninsula and threatening the stability of the West Antarctic Ice Sheet, together with the urgency in predicting future ice loss (e.g. Mouginot et al., 2014; Golledge et al., 2015; DeConto and Pollard, 2016; Gardner et al., 2018; Seroussi et al., 2020; Levermann et al., 2020), it is essential, beyond the legal imperative stated in Section III 1-c of the Antarctic Treaty, for these data to be freely available to the international community.

Supported by the Scientific Committee of Antarctic Research (SCAR) Bedmap3 Action Group, this paper presents the release of all of the underlying ice bed, surface, and thickness survey data points that have been used in the previous and upcoming versions of Bedmap gridded products (Bedmap1, Bedmap2, and Bedmap3). We discuss the standardization of the data following the Findable, Accessible, Interoperable, and Reusable (FAIR) data principles (Wilkinson et al., 2016) and the use of consistent data formats and attributes, as agreed to by the international community through the Bedmap project. Additionally, we introduce the SCAR Bedmap Data Portal (https://bedmap.scar.org, last access: 1 March 2023), which offers the ability to search individual datasets within one stand-alone map-based platform and increases the discoverability and accessibility of the data. Our aim is to make the gridding process as reproducible as possible by making the source survey data fully standardized, openly available, and easily accessible through one portal. It is expected that the data presented in this paper will facilitate the creation of a range of new gridded products at different spatial resolutions, enable the application of emerging techniques such as machine-learning and geostatistical techniques to fill gaps between direct measurements, and provide a common data-sharing baseline for future geophysical surveying of Antarctica. A follow-up publication to this paper will introduce the new gridded products from Bedmap3.

Section 2 of this paper discusses the background and evolution of past surveying of Antarctica using geophysical techniques. Section 3 presents how the source data have been standardized. Section 4 details how the data are published following the FAIR data principles.

2 Background: evolution of the Bedmap products

2.1 1950–1980: first geophysical measurements of ice thickness in Antarctica

Prior to the start of radio-echo-sounding (RES) measurements over Antarctica, ice thickness was primarily obtained from seismic techniques (Schroeder et al., 2020). RES was developed in the 1950s after studying the transparency of ice to specific radio frequencies and the realization of its potential for glaciological research by Armory Waite and Stanley Evans (Turchetti et al., 2008). After several years of developments and tests, the first long-range airborne radio-echo sounding of the Antarctic Ice Sheet was undertaken by the Scott Polar Research Institute (SPRI), with support from the United States National Science Foundation and the Technical University of Denmark in the late 1960s (Robin et al., 1970). By 1975, the elevation data from the 1971–1975 Antarctic field seasons were compiled into a series of topographic maps of Antarctica (Drewry, 1975). These became the first comprehensive topographic maps of the Antarctic continent and would lead to more sophisticated compilation grids in the following years.

2.2 1980–1990: first compilation efforts to map Antarctica

By 1983, around 50 % of the Antarctic Ice Sheet had at least some airborne RES survey measurements (i.e. within a 50 to 100 km square grid cell) (Drewry et al., 1982), and the first compilation bed elevation map was published. Sheets 3

and 4 in the SPRI Glaciology and Geophysical Folio Series (Drewry, 1983) became a reference for bedrock surface and ice thickness for Antarctica. The grid contours of bed elevation were drawn from ice thickness data collected on sparse surface traverses and by airborne surveys over the entire continent using state-of-the-art digital-mapping techniques, although in many areas survey lines were separated by hundreds of kilometres (Lythe and Vaughan, 2000).

2.3 1990–2020: the Bedmap era

In the mid-1990s, advances in radar data acquisition and development of modern global navigation satellite systems (GNSSs) led to substantial improvements in the coverage and accuracy of the data collected. Until then the positioning was often inferred using the "unaided inertial navigation" technique which often had substantial positioning errors (Schroeder et al., 2020).

In 1996, the first BEDMAP consortium group (here termed Bedmap1) was set up under the joint sponsorship of the European Ice Sheet Modelling Initiative (EISMINT) and SCAR. It led to the publication of the first Bedmap products: a printed map published in 2000 (Lythe and Vaughan, 2000) and its associate digital version in 2001 (Lythe and Vaughan, 2001). For more than a decade, Bedmap1 played a crucial role in providing large-scale boundary conditions of the Antarctic Ice Sheet for observational and modelling applications (e.g. Pollard and DeConto, 2009; Shepherd et al., 2012). The gridded map contained ice thickness data from direct measurements, including ground-based and airborne RES but also from seismic and gravimetric measurements (Lythe and Vaughan, 2001). Although pioneering, this first gridded product had a relatively low resolution of 5 km and suffered from large data gaps, particularly over East Antarctica, which resulted in low-confidence values in those areas (see Fig. 1a).

Motivated by a wealth of newly acquired data over Antarctica and improved geographic information system techniques, the second version of Bedmap was published in 2013 (Fretwell et al., 2013). The Bedmap2 product was composed of several grids including ice bed, surface, and thickness data for Antarctica and their associated uncertainties, in addition to several masks (e.g. continental ice edge, grounding line, ice shelf extent) useful for ice sheet modelling. This compilation included 25 million measurements, an order of magnitude more than were used in Bedmap1. This time, the ice thickness, bed elevation, and surface elevation grids were provided at a uniform 1 km spacing but still with a native interpolation resolution of 5 km to satisfy the data providers' conditions for use (Fretwell et al., 2013).

Since 2012, new RES datasets have been collected across Antarctica, with a particular focus on the "poles of ignorance" identified in Bedmap2 (Pritchard, 2014), thus filling known data gaps in key areas of East Antarctica (see Sect. 3.1). In addition, new hybrid compilation efforts such as BedMachine Antarctica have used a combined modelling–observation approach, including a mass conservation method, to generate improved bed topography and ice thickness in data-deficient areas of the Antarctic coastline (Morlighem et al., 2020).

2.4 2020–present: general approach for Bedmap3

In 2020, the SCAR Bedmap3 Action Group was tasked with producing an updated version of the Bedmap gridded products and with improving the accessibility of the underlying survey datasets of Antarctic ice thickness and bed topography (see Fig. 1a–c) through standardization and dissemination of the data via the new SCAR Bedmap Data Portal. This will serve as a common endpoint to discover and interact with all underlying Bedmap data.

The Bedmap3 gridded products will be constructed using a similar process to Bedmap2 but will offer a significant improvement in survey data coverage along with a newly updated grounding line, updated altimetry-derived surface topography, and updated ice extent and bathymetry. Each iteration of Bedmap contains large survey data additions that have increased the accuracy of the gridded products. In total, Bedmap3 contains 82 million points and thus includes twice the number of new data points available to Bedmap2 (Fig. 1d, Tables 1 and S2).

3 Source data, standardization and pre-processing

3.1 Ice thickness, surface and bed elevation data

The primary source data consist of survey point measurements of ice thickness, bed elevation and surface elevation, which principally come from airborne radar surveys and seismic soundings and to a smaller extent from ground-based radar surveys. We present here the data compiled within each version of Bedmap.

Bedmap1 source data (1950s–1990s) often lack the campaign metadata available for more modern datasets, and so we present these as a single dataset. In total, the data standardized for Bedmap1 consist of almost 2 million points from 127 individual campaigns (Table 1). While the data coverage is substantial, especially over West Antarctica and the Antarctic Peninsula (Fig. 1a), the distance between individual flight lines and soundings is much larger than those of the Bedmap2 and Bedmap3 data. In addition, though efforts continue to leverage modern data to improve the geometric, positioning, and radiometric calibration for these archival data, the spatial accuracy of the survey data is poorer due to the use of older navigation techniques prior to the GNSS era (see Schroeder et al., 2019, 2021).

Additional Bedmap2 source data were acquired from 2000 to 2012 by 66 new surveys that contributed a further 27 million points (Table S1), filling major gaps over West Antarctica's fast-flowing ice streams such as the Pine Is-

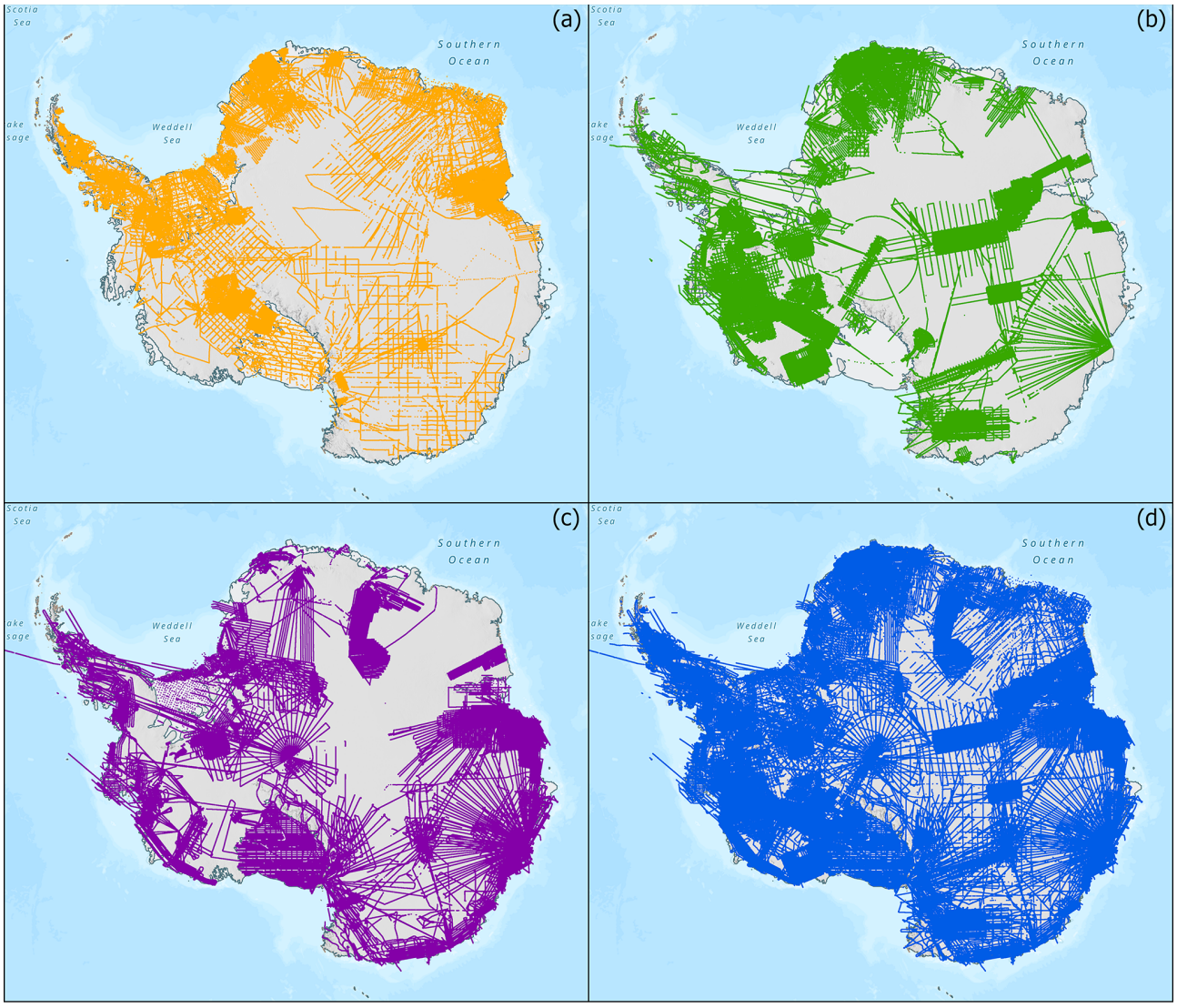

Figure 1. Data coverage for the three generations of Bedmap products. **(a)** Data coverage for Bedmap1. **(b)** Additional data coverage for Bedmap2. **(c)** Additional data coverage for Bedmap3. **(d)** Total combined coverage now available.

land (Vaughan et al., 2006) and Thwaites (Holt et al., 2006) glaciers as well as over East Antarctica's Gamburtsev Subglacial Mountains (Sun et al., 2009; Bell et al., 2011; Ferraccioli et al., 2011) and Wilkes Subglacial Basin (Frederick et al., 2016) (Fig. 1b).

Further new data available to Bedmap3 come from 84 new surveys by 15 data providers, representing an additional 52 million data points and 1.9 million line kilometres of measurements (Table S2). These latest data have filled major gaps, particularly in the key sector of East Antarctica, including the South Pole (Jordan et al., 2018) and Pensacola basin (Paxman et al., 2019), Dronning Maud Land, Recovery Glacier (Forsberg et al., 2017) and Dome Fuji (Eagles et al., 2018; Karlsson et al., 2018), and Princess Elizabeth Land (Cui et al., 2020; Popov, 2020). Additional data covering glacier troughs and floating ice shelves give insights into previously undersampled sectors, such as over the Antarctic Peninsula, West Antarctic coastlines, or the Transantarctic Mountains as part of NASA Operation IceBridge (MacGregor et al., 2021).

3.2 Standardization

Due to the large number of data providers and the lack of common protocols, the data received as part of Bedmap data calls came in various forms, including text, comma-separated value (CSV), ASCII or Excel files. To ensure long-term accessibility, all submitted data files were standardized based

Table 1. Comparison of data campaigns and coverage of the different Bedmap generations.

Bedmap version	Cumulative campaigns	Cumulative data points	Cumulative dataset volume
Bedmap1	127	2 million	213 MB
Bedmap2	193	29 million	7.2 GB
Bedmap3	277	82 million	22.8 GB

upon a template agreed to by the SCAR Action Group and converted to a specific CSV format. Open and easy to use, this format has been widely used in the scientific community and is well suited for storing tabular data.

As an ASCII-delimited file, the CSV format allows long-term preservation of the data thanks to its very simple structure. This format is often recommended (e.g. https://www.gov.uk/government/publications/recommended-open-standards-for-government/tabular-data-standard, last access: 1 March 2023, UK Government, 2020), but no strict definition exists. One common definition is the RFC 4180 definition (https://www.ietf.org/rfc/rfc4180.txt, last access: 1 March 2023, IETF RFC 4180, 2005), which describes the CSV format as tabular data with zero to one header rows, followed by the same number of fields separated by commas. With only one row header, the metadata allowed by this definition are extremely poor. To add information, a solution is to repeatedly add the metadata to each data row but at the cost of greatly increasing the file size. That is why the CSV on the Web (CSVW) standard developed by the W3C working group (https://www.w3.org/TR/tabular-data-primer/, last access: 1 March 2023, CSV on the Web, 2016) or NCCSV, a NetCDF-compatible ASCII CSV file (https://coastwatch.pfeg.noaa.gov/erddap/download/NCCSV.html, last access: 1 March 2023, NCCSV, 2023) developed by NOAA, recommend adding the metadata or notes in a separated JSON or CSV file. Although the metadata as described by the CSVW or NCCSV recommendations are excellent in terms of machine readability, the metadata are hidden in a complicated structure that compromises human readability. For this reason, we used an extended version of CSV that purposely does not follow the RFC 4180 definition but provides the possibility of adding metadata in the data file itself. Different definitions of such a format exist, such as the geoCSV format developed within the GeoWS project (http://geows.ds.iris.edu/documents/GeoCSV.pdf, last access: 1 March 2023, IRIS, 2015) or the extCSV format recommended by the World Ozone and Ultraviolet Radiation Data Centre (https://woudc.org/about/formats.php, last access: 1 March 2023, Canada World Ozone and Ultraviolet Radiation Data Centre, 2023).

The format used for the Bedmap Data Portal follows most of the geoCSV recommendations, and headers are compliant with the Climate and Forecast (CF) Metadata Conventions (https://cfconventions.org/, last access: 1 March 2023, Hassell et al., 2017) and include recommended attributes from the Attribute Convention for Data Discovery (ACDD, https://wiki.esipfed.org/Attribute_Convention_for_Data_Discovery_1-3, last access: 1 March 2023, Earth Science Information Partners, 2023). As part of the standardization, a specific header and structure consisting of identical variable names in a strict order for all the ice thickness data were developed in order to simplify access, particularly for programming purposes. The format consists of (i) an extended header section, (ii) a header row composed of the column name following the CF convention and units in parentheses, and finally (iii) the data using a comma as the separator. The extended header consists of general information regarding each campaign, such as the year, the name of the main investigator, and funding and processing details as shown in Table 3. The complete list and order of the attributes and variables are given in Table 2.

The developed format is machine-readable, making the conversion of the files to CSVW or NCCSV standards straightforward if necessary.

3.3 Summarized point data

In addition to providing standardized CSV data (see Sect. 3.1), we also provide the data as shapefile and geopackage lines and statistically summarized points. Lines were calculated automatically from the point data and split each time a gap of more than 5 km between two data points was found. For Bedmap1, due to the sparsity of points, it was not possible to convert the data to shapefile or geopackage lines; thus, only the Bedmap1 shapefile points are provided as part of this data release. Please also note that the Bedmap1 data are not split per campaign as per Bedmap2 and Bedmap3 and are only provided as a single geopackage or as shapefile point files.

The spatial distribution of the full-resolution survey point data is heterogeneous with, for example, dense, metre-scale sampling along modern flight lines that are often separated across-track by kilometres to hundreds of kilometres, and this heterogeneity varies between campaigns and data providers. Uneven data distribution can cause gridding algorithms to be overly weighted to those areas with the highest sampling frequency, to the detriment of adjacent areas with valid data but sparser sampling. To reduce the impact of

Table 2. List of variable and attribute names provided in the CSV files. To guarantee the machine readability of the variable names, the use of special characters was avoided. Conventions include the CF convention (https://cfconventions.org/, last access: 1 March 2023, Hassell et al., 2017) and recommended attributes from the Attribute Convention for Data Discovery (ACDD, https://wiki.esipfed.org/Attribute_Convention_for_Data_Discovery_1-3, last access: 1 March 2023, Earth Science Information Partners, 2023).

Variable or attribute name	Unit	Details	Convention
Extended header information			
project		Name of the project or campaign name	ACDD
time_coverage_start	Year	Start time of acquisition	ACDD
time_coverage_end	Year	End time of acquisition	ACDD
creator_name		Name of contact person or institute responsible for the creation of the dataset	ACDD
institution		The name of the institution principally responsible for originating these data	ACDD, CF
acknowledgement		Name of the funding agency	ACDD
source		Digital object identifier for where the original data are deposited	ACDD, CF
references		References pointing to the main publication or discussion of the dataset	ACDD
platform		Type of platform used for the survey: ground-based radar, airborne radar or seismic	CF
instrument		Name of the instrument system used for the acquisition	ACDD
history		Acquisition or processing lineage information	ACDD
electromagnetic_wave_speed_in_ice	Metres/microseconds ($m\,\mu s^{-1}$)	Electromagnetic wave speed in ice	
firn_correction	Metres (m)	Firn correction	
centre_frequency	MegaHertz (MHz)	Centre frequency	
comment		Comment section used to give the Bedmap version	ACDD, CF
metadata_link		Link to the Bedmap digital object identifier	ACDD
license		URL of the license used	ACDD
conventions		Name of the conventions used	ACDD
Variable names			
trajectory_id		Line or flight ID	CF
trace_number		Trace number from the specific line given in Line_ID	
longitude	Decimal degrees (east)	Longitude (WGS84 EPSG: 4326)	CF
latitude	Decimal degrees (north)	Latitude (WGS84 EPSG: 4326)	CF
date	YYYY-MM-DD	Date following the ISO 8601 format: YYYY: year, MM: month, DD: day	
time_UTC	HH:MM:SS	UTC time following the ISO 8601 format: HH: hours, MM: minutes, SS: seconds	
surface_altitude	Metres (m)	Surface elevation or altitude (referenced to WGS84)	CF
land_ice_thickness	Metres (m)	Ice thickness	CF
bedrock_altitude	Metres (m)	Bed elevation or altitude (referenced to WGS84)	CF
two_way_travel_time	Seconds (s)	Two-way travel time	
aircraft_altitude	Metres (m)	Aircraft elevation or altitude to bedrock when applicable (referenced to WGS84)	
along_track_distance	Metres (m)	Distance in the along-track direction	

data density on gridding, the statistically summarized shapefile/geopackage point dataset (centred on a continent-wide 500 m × 500 m grid) reports the average values of the full-resolution survey data plus information on their distribution (Table 4). These summary statistics enable assessment of the confidence in the averaged data values and the variability of the measurements within each cell (e.g. bed roughness). Figure 2 gives an insight into the mean values of ice thickness, bed elevation, and surface elevation as well as the number of points per cells used for the calculation.

Table 3. Example of header information provided for the 2018 Thwaites Glacier radar data. The extended header section can be described as follows: (a) each line is introduced by a comment ("#") character, (b) each line contains a single header item, (c) the colon character (":") is used as the key/value separator, (d) units are in parentheses and (e) attributes preferably use a common vocabulary such as the CF convention and include attributes from the ACDD.

```
#project: Thwaites Glacier (ITGC).
#time_coverage_start: 2018
#time_coverage_end: 2019
#creator_name: British Antarctic Survey.
#institution: British Antarctic Survey.
#acknowledgement: NERC/NSF International Thwaites Glacier Collaboration (ITGC).
#source: https://data.cresis.ku.edu/
#references: https://doi.org/10.5194/tc-14-2869-2020
#platform: airborne radar.
#instrument: PASIN.
#history: 2-D synthetic aperture radar processing
#electromagnetic_wave_speed_in_ice: 168 (metres/microseconds)
#firn_correction: 10 m
#centre_frequency: 150 MHz
#comment: part of Bedmap3
#metadata_link: https://doi.org/10.5285/91523ff9-d621-46b3-87f7-ffb6efcd1847
#license: https://creativecommons.org/licenses/by/4.0/
#Conventions: ACDD-1.3, CF-1.8
```

The links provided in the table below were last accessed on 29 May 2023.

Table 4. List of summary statistics calculated for each shapefile point. For each variable, we provide its short name, long name and associated unit when applicable. These statistics are calculated for each point of the shapefile point file.

Short name	Long name	Units
Cnt_bed	Number of points for bed elevation	–
Cnt_surf	Number of points for surface elevation	–
Cnt_thick	Number of points for ice thickness	–
IQR_bed	Interquartile range for bed elevation points	Metres
IQR_surf	Interquartile range for surface elevation points	Metres
IQR_thick	Interquartile range for ice thickness points	Metres
Max_bed	Maximum value of bed elevation	Metres
Max_surf	Maximum value of surface elevation	Metres
Max_thick	Maximum value of ice thickness	Metres
Mean_bed	Mean value of bed elevation	Metres
Mean_dist	Mean distance between cell centre and points	Metres
Mean_surf	Mean value of surface elevation	Metres
Mean_thick	Mean value of ice thickness	Metres
Med_bed	Median value of bed elevation	Metres
Med_surf	Median value of surface elevation	Metres
Med_thick	Median value of ice thickness	Metres
Min_bed	Minimum value of bed elevation	Metres
Min_surf	Minimum value of surface elevation	Metres
Min_thick	Minimum value of ice thickness	Metres
SD_bed	Standard deviation of bed elevation	Metres
SD_surf	Standard deviation of surface elevation	Metres
SD_thick	Standard deviation of ice thickness	Metres
STE_bed	Standard error of bed elevation	Metres
STE_surf	Standard error of surface elevation	Metres
STE_thick	Standard error of ice thickness	Metres

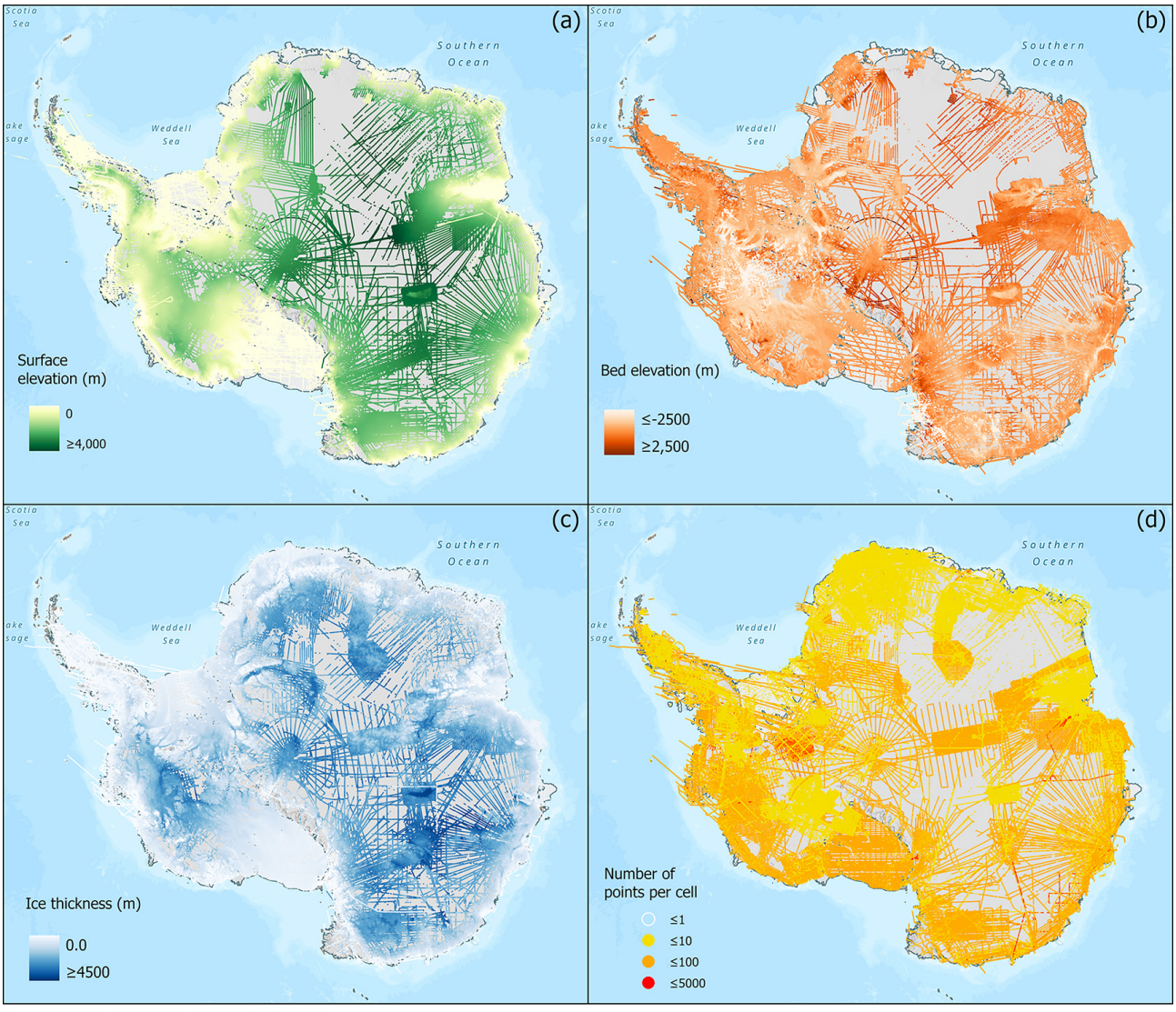

Figure 2. Statistically summarized data points. **(a)** Mean surface elevation in metres over Antarctica. **(b)** Mean bed elevation in metres over Antarctica. **(c)** Mean ice thickness in metres over Antarctica. **(d)** Number of points per cell used for the calculation of ice thickness. All elevation values in panels **(a)**–**(b)** are given with reference to the WGS84 ellipsoid.

3.4 Quality control and limitations

The purpose of this data release is to include all possible data collected over the last 60 years without discriminating the quality of the data. Data have been directly compiled from the data providers, with only minimal quality checks: all non-value data were converted to −9999, including any negative ice thickness values and any points with clear outliers. We checked the minimum and maximum values of each field to ensure the data are in a reasonable range and calculated the mean and standard deviation on each dataset to identify potential issues. For example, if longitude–latitude values did not fall within the expected −180 to 180° or −50 to −90° ranges respectively, the entire row was removed. When no ice thickness values were provided but surface and bed elevation values existed, we simply calculated ice thickness by subtracting the surface value from the bed value. At times, bed elevation was higher than surface elevation, likely due to issues with the semi-automatic picker used to extract the surface and bed reflector or a lack of distinctive reflectors in areas of shallow ice. To prevent this from affecting the gridded product, we converted these values to −9999 for both the surface and the bed. Finally, we also conducted routine checks on the ice thickness data by comparing the given ice thickness value with the inferred ice thickness calculated from subtracting surface with bed. If these did not match, we placed −9999 on the ice thickness values.

File-naming conventions were also used throughout to easily identify a specific dataset as follows: DataProvider_Year_CampaignName_TypeofData_BM3. The type of data used were separated into three categories: airborne radar (AIR), ground-based radar (GRN), and seismic (SEI) data. The "BM3" abbreviation at the end identifies the datasets as part of the Bedmap3 compilation to differentiate them from the Bedmap1 and Bedmap2 (BM1 and BM2) compilations. For instance, the file named "NASA_2019_ICEBRIDGE_AIR_BM3.csv" refers to the ICEBRIDGE airborne campaign led by NASA in 2019. Providing an overall uncertainty value for all the bed elevations compiled by Bedmap is challenging due to the number of data providers and radar systems used in the last 60 years (see the Appendix tables). This uncertainty is often calculated as the root-mean-square error (RMSE) of bed elevation values at crossover points across a survey area (e.g. Fremand et al., 2022a). This error typically amounts to tens of metres and is constrained by changing bed characteristics, the radar system used, the processing of the data, and the value used for the propagation of radar waves through ice which is used to convert the radar two-way travel time to depth in metres. The metadata compiled by Bedmap for each survey provide information on whether any firn correction has been applied to the elevation values and on the value used for speed of electromagnetic waves through the ice.

In order to address the uncertainty in elevation values for the entire Bedmap dataset, we provide standard deviation, interquartile range, and standard error statistical parameters which are key to determining the variability of values in each 500 m × 500 m cell. The standard deviation represents the typical deviation of each data point to the mean value of the specific cell and thus can be used to assess how accurately the mean value is representative of the real values. The standard error gives information about the variability across all the data points in the specific cell and is used to estimate how well a specific data point is representative of the whole population. A high standard error indicates that the data within a specific cell are widely spread around the population mean. The interquartile range calculates the difference between the first quartile and the third quartile and is used to measure the variability of the middle 50 % of all the values. In contrast to the standard error and standard deviation, the interquartile range is not affected by extreme outliers that are present in a specific cell. Together, these parameters are used to assess the level of confidence in the data, where low values reflect a stronger fidelity in the data.

We also note that the spatial accuracy of datasets included in Bedmap2 and Bedmap3 is significantly higher than for Bedmap1 due to the use of high-resolution GPS data, which have allowed for much better accuracy in the location of the measurements for all surveys acquired from the 1990s onwards. The accuracy of each bed elevation or ice thickness value can vary from sub-metre accuracy for modern GPS measurements (Fremand et al., 2022a) to several kilometres for data compiled as part of the Bedmap1 dataset (Schroeder et al., 2019). As this spatial uncertainty directly impacts the position of the elevation values and therefore their accuracy, the elevation uncertainty statistical parameters can be used to indirectly assess the confidence in the spatial accuracy. However, the statistical parameters are only meaningful if a representative set of points is used to calculate the ice thickness, bed elevation, and surface elevation.

As part of the follow-up publication to this paper introducing the new Bedmap3 gridded products, we will include the final grids and maps that will study and exclude possible crossover errors and other possible problems in order to provide high-quality gridded products.

4 Publishing the Bedmap source data

The Bedmap source data are available via the UK Polar Data Centre (PDC, https://www.bas.ac.uk/data/uk-pdc/, last access: 1 March 2023), a trusted repository whose purpose is to manage polar datasets. Part of the Environment Data Services (EDS) of the Natural Environment Research Council (NERC) and certified by the CoreTrustSeal (https://www.coretrustseal.org/, last access: 1 March 2023), the PDC applies best data management practices and requirements to facilitate re-use of the datasets stored in its data catalogue (https://data.bas.ac.uk/, last access: 1 March 2023). To increase the discoverability of the datasets, a specific data portal – the SCAR BEDMAP Data Portal (https://bedmap.scar.org, last access: 1 March 2023) – has been developed by the Mapping And Geographic Information Centre (MAGIC) team from the British Antarctic Survey (BAS). The publishing procedure described here is expected to be used for all upcoming versions of Bedmap with regular updates allowing new source data to be easily accessible to the community.

Below, we discuss the release of the datasets centred around the FAIR data principles (Sect. 4.1) and present the data portal infrastructure and its functionalities (Sect. 4.2).

4.1 FAIR data publishing

The source data for each version of Bedmap have been published as two separate digital object identifier (DOI) datasets: the first dataset contains all the standardized CSV files described in Sect. 3.1, and the second dataset contains all the lines and point shapefiles as discussed in Sect. 3.2.

The derived gridded Bedmap products are also published as separate DOI datasets. Previously available through ftp services, Bedmap1 and Bedmap2 products are now citable and properly stored for long-term preservation. Table 5 presents the different links to the data for the different versions of Bedmap.

To make the data findable, ISO 19115/19139 metadata are provided for each dataset. Each metadata record provides general information about the dataset and is registered and indexed accordingly in the UK PDC data catalogue

Table 5. List of references for the Bedmap products. For each Bedmap product (Bedmap1, Bedmap2, and Bedmap3), we provide the link to the standardized CSV and shapefile data.

Bedmap version	Standardized CSV	Shapefile points
Bedmap1	https://doi.org/jg6q (Lythe et al., 2022a)	https://doi.org/jg6s (Lythe et al., 2022b)
Bedmap2	https://doi.org/jg6r (Fretwell et al., 2022a)	https://doi.org/jg6t (Fretwell et al., 2022b)
Bedmap3	https://doi.org/jg6n (Fremand et al., 2022b)	https://doi.org/jg8b (Fremand et al., 2022c)

Discovery Metadata System (https://data.bas.ac.uk/, last access: 1 March 2023) and the NERC data catalogue (https://data-search.nerc.ac.uk/, last access: 1 March 2023). More detailed information can be found in the extended header of the CSV data, such as the name of the data providers, the funding received, and a reference to cite the data. Although the metadata are succinct, it is possible to easily transform the CSV data to NetCDF with extended metadata as shown in the Geophysics Book (https://antarctica.github.io/PDC_GeophysicsBook/BEDMAP/Get_full_metadata_from_CSV_file.html, last access: 1 March 2023).

A DOI is provided for every Bedmap dataset (Table 5), making them retrievable and citable. For previously published datasets, the original DOI is provided in the source metadata (Sect. 3.2) to ensure traceability and should be used when the survey is used individually.

For universal accessibility, the data are downloadable through a standard HTTPS protocol where no login account is required. We used the web-based RAMADDA (Repository for Archiving and MAnaging Diverse DAta; https://geodesystems.com/, last access: 5 May 2023) data repository system, which is an open-source content and data management platform and which works following a simple folder structure, with datasets organized by data-provider name to replicate the structure of the data portal.

To enhance interoperability and reusability, we published the underlying data using a specific CSV format, with detailed and standardized variable names coming from FAIR vocabularies (see Table 4 and Sect. 3.2). To be re-usable, the data are released under Creative Commons license CC-BY (https://creativecommons.org/licenses/by/4.0/, last access: 1 March 2023, Creative Commons – Attribution 4.0 International – CC BY 4.0, 2023), which allows any user to use the data freely and with flexibility while at the same time ensuring acknowledgment of those involved in the collection and processing of the data. Keywords from the Global Change Master Directory (GCMD, 2023) are used to describe the data in a consistent and comprehensive manner and to increase the interoperability of the datasets. The end goal is to provide all the information necessary for effective, long-term data re-use. In addition, we developed interactive, open-source Jupyter Notebook tutorials written in Python to interact with the data programatically. Codes to convert the standardized CSV files to the point and line files as described in Sect. 3.3 are provided for example. These resources are archived in the BAS GitHub repository and provided via an interactive web interface using Jupyter Book (https://antarctica.github.io/PDC_GeophysicsBook, last access: 1 March 2023, UK Polar Data Centre, 2023a). In addition, a specific Python package allows one to read and plot the specific CSV-formatted data (https://github.com/paul-breen/xcsv, last access: 5 May 2023, Breen, 2023). We believe these to be beneficial for assisting users in accessing the data and reproducing their own gridded products independently of the Bedmap project.

4.2 The SCAR Bedmap Data Portal

The newly developed SCAR Bedmap Data Portal (https://bedmap.scar.org, last access: 1 March 2023) provides a common endpoint for interacting with the Bedmap source data and products. The web-map architecture is based upon the well-used SCAR Antarctic Digital Database web map (https://add.scar.org, last access: 1 March 2023). The data portal is divided into five layer menus: “Base layers”, “Topographic information”, “BEDMAP1”, “BEDMAP2”, and “BEDMAP3”. The first menu contains the gridded products: ice bed, surface, and thickness grids for Antarctica currently contain Bedmap2 grids; these will be updated with new Bedmap3 grids as they become available. The second menu contains general topographic information such as coastline and ice–land surface contours taken from the Antarctic Digital Database (Gerrish et al., 2023). The three Bedmap tabs contain the shapefile layers for individual campaigns. When clicking on a point of the map, the user has direct access to the information of the survey and statistics for the specific point (see Table 4).

At the top of the interface, several widgets are available, designed to help users with basic tasks such as measuring distances, areas, and elevations or to search for specific place names. The link to the direct download repository is also provided.

5 Data availability

All the data included in this paper are freely available from the UK Polar Data Centre (https://data.bas.ac.uk, last access: 1 March 2023) and the SCAR Bedmap Data Portal (https://bedmap.scar.org, last access: 1 March 2023).

BEDMAP1:

– https://doi.org/jg6q (Lythe et al., 2022a);

– https://doi.org/jg6s (Lythe et al., 2022b);

– https://doi.org/j2vz (Lythe et al., 2023).

BEDMAP2:

– https://doi.org/jg6r (Fretwell et al., 2022a);

– https://doi.org/jg6t (Fretwell et al., 2022b);

– https://doi.org/jg6p (Fretwell et al., 2022c).

BEDMAP3:

– https://doi.org/jg6n (Fremand et al., 2022b);

– https://doi.org/jg8b (Fremand et al., 2022c).

The data can be downloaded directly from the RAMADDA interface by clicking on the "GET DATA" link from the metadata page or using wget commands as documented in the following instructions: https://antarctica.github.io/PDC_GeophysicsBook/BEDMAP/Downloading_the_Bedmap_data.html (last access: 1 March 2023, UK Polar Data Centre, 2023b).

When using these data, please also cite the DOI citation provided in the source CSV metadata if this exists.

6 Code availability

The user guide for the data portal and the Jupyter Notebook tutorials designed for reading the standardized CSV ice bed, elevation, and thickness data or creating the shapefiles are accessible on the Jupyter Book interface in the BEDMAP3 section (https://antarctica.github.io/PDC_GeophysicsBook, last access: 1 March 2023, UK Polar Data Centre, 2023a) or via the BAS GitHub repository (https://github.com/antarctica/PDC_GeophysicsBook, last access: 1 March 2023; DOI: https://doi.org/10.5281/zenodo.7821671, Fremand, 2023). A specific library called xcsv (https://github.com/paul-breen/xcsv, last access: 1 March 2023, Breen, 2023, last access: 1 March 2023) allows one to read and plot data in the extended CSV format as described in Section 3.2.

7 Conclusion

We have presented here the release of the source survey data on ice thickness, bed elevation, and surface elevation data used in Bedmap gridded products, including the upcoming Bedmap3. Altogether, this data release represents over 82 million data points collected as part of 277 campaigns since the 1950s. In addition to the previous Bedmap1 and Bedmap2 datasets, here we have gathered new ice thickness data from 84 surveys, adding 50 million additional data points to those previous compilations. We have developed a standardized CSV format in order to ensure interoperability between the different datasets, which we have checked following a specific quality-control procedure and summarized on a 500 m × 500 m grid to provide key statistics at the scale needed for the Bedmap3 gridded products.

The data have been published following the FAIR data principles. In particular, we have provided extensive metadata with commonly used keywords and have developed a data portal that provides a user-friendly interface to interact with and download the data. By providing and displaying both the source data and grids, the data portal allows any user to investigate the uncertainty of the gridding in specific areas and analyse differences between measurements and gridded interpolations.

We believe that this data release will benefit the glaciology and broader Earth science community, particularly in emerging fields such as machine learning and geostatistics which can now make use of these standardized data and reproduce and create new compilation grids at different scales independently of the Bedmap grids. These standardized, freely available, and previously unpublished datasets will lead to improved assessment of fundamental properties of the Antarctic Ice Sheet and predictions of its future contribution to sea level rise, increasing the value of these important data.

Supplement. The supplement related to this article is available online at: https://doi.org/10.5194/essd-15-2695-2023-supplement.

Author contributions. ACF, PF, and JAB co-led this data release. ACF and JAB standardized the data. The Jupyter Notebook was developed by ACF. PF and HDP initiated the collaboration and PF liaised with all the data providers. ACF wrote the initial manuscript with input from PF, JAB, and HDP. PF designed and populated the web map. EF helped with the design of the web map.

AA, BS, OE, PF, JG, JL, KM, MM, FP, SVP, HDP, ACF, JAB, JR, DMS, MJS, DS, KT, XC, and DAY were all members of the Bedmap3 SCAR Core Group and contributed to the overall project and standardization criteria.

PF, HDP, AA, JLB, RB, CB, RGB, DDB, GCas, GCat, KC, HC, HFJC, XC, DD, VD, RD, GE, OE, HE, FF, RF, StF, ShF, YG, VG, SPG, JG, BH, RCAH, AOH, PH, NH, JWH, ANH, AH, RWJ, DJ, AJ, WJ, TJ, EK, JK, WK, MKG, KL, JL, GL, CL, BL, JMa, EM, KM, JMo, FON, YN, OAN, JP, FP, SVP, ER, DMR, ARi, JR, NR, ARu, DMS, MJS, AMS, DS, MS, BS, IT, KT, SU, DV, BCW, DSW, DAY, and AZ contributed to the data. All the authors commented on and contributed to the final edits of the manuscript prior to publication.

Competing interests. At least one of the (co-)authors is a member of the editorial board of *Earth System Science Data*. The peer-review process was guided by an independent editor, and the authors also have no other competing interests to declare.

Disclaimer. Publisher's note: Copernicus Publications remains neutral with regard to jurisdictional claims in published maps and institutional affiliations.

Acknowledgements. We would like to thank the Bedmap3 SCAR Action Group for their role in the coordination and guidance in the project.

We would like to dedicate this paper to the many scientists who have collected geophysical field data in harsh and extreme conditions over the Antarctic ice sheets over the last 60 years. Their commitment, dedication, and drive have populated this dataset and have greatly advanced polar science.

Funding for the British Antarctic Survey staff came from Natural Environment Research Council core funds.

Funding for the data collection came from many grants, institutions, and projects. These are individually cited where appropriate in the metadata of the datasets.

Financial support. This research has been supported by the Natural Environment Research Council (grant no. NE/R016038/1).

Review statement. This paper was edited by Ken Mankoff and reviewed by Johnathan Kool and one anonymous referee.

References

Bell, R. E., Ferraccioli, F., Creyts, T. T., Braaten, D., Corr, H., Das, I., Damaske, D., Frearson, N., Jordan, T., Rose, K., and Studinger, M.: Widespread persistent thickening of the East Antarctic Ice Sheet by freezing from the base, Science, 331, 1592–1595, https://doi.org/10.1126/science.1200109, 2011.

Breen, P.: xcsv, GitHub [code], https://github.com/paul-breen/xcsv, last access: 1 March 2023.

Canada World Ozone and Ultraviolet Radiation Data Centre: File formats, https://woudc.org/about/formats.php, last access: 1 March 2023.

Creative Commons – Attribution 4.0 International – CC BY 4.0: https://creativecommons.org/licenses/by/4.0/, last access: 1 March 2023.

CSV on the Web: A Primer, https://www.w3.org/TR/tabular-data-primer/ (last access: 29 July 2022), 2016.

Cui, X., Jeofry, H., Greenbaum, J. S., Guo, J., Li, L., Lindzey, L. E., Habbal, F. A., Wei, W., Young, D. A., Ross, N., Morlighem, M., Jong, L. M., Roberts, J. L., Blankenship, D. D., Bo, S., and Siegert, M. J.: Bed topography of Princess Elizabeth Land in East Antarctica, Earth Syst. Sci. Data, 12, 2765–2774, https://doi.org/10.5194/essd-12-2765-2020, 2020.

DeConto, R. M. and Pollard, D.: Contribution of Antarctica to past and future sea-level rise, Nature, 531, 591–597, https://doi.org/10.1038/nature17145, 2016.

DeConto, R. M., Pollard, D., Alley, R. B., Velicogna, I., Gasson, E., Gomez, N., Sadai, S., Condron, A., Gilford, D. M., Ashe, E. L., Kopp, R. E., Li, D., and Dutton, A.: The Paris Climate Agreement and future sea-level rise from Antarctica, Nature, 593, 83–89, https://doi.org/10.1038/s41586-021-03427-0, 2021.

Drewry, D. J.: Radio echo sounding map of Antarctica, (∼ 90° E–180°), Polar Rec., 17, 359–374, https://doi.org/10.1017/S0032247400032186, 1975.

Drewry, D. J.: Antarctica: glaciological and geophysical folio, University of Cambridge, Scott Polar Research Institute Cambridge, UK, ISBN 0-901021-04-0, 1983.

Drewry, D. J., Jordan, S. R., and Jankowski, E.: Measured Properties of the Antarctic Ice Sheet: Surface Configuration, Ice Thickness, Volume and Bedrock Characteristics, Ann. Glaciol., 3, 83–91, https://doi.org/10.3189/S0260305500002573, 1982.

Eagles, G., Karlsson, N.B., Ruppel, A., Steinhage, D., Jokat, W., and Läufer, A.: Erosion at extended continental margins: Insights from new aerogeophysical data in eastern Dronning Maud Land, Gondwana Res., 63, 105–116, https://doi.org/10.1016/j.gr.2018.05.011, 2018.

Earth Science Information Partners: Attribute Convention for Data Discovery 1–3, https://wiki.esipfed.org/Attribute_Convention_for_Data_Discovery_1-3, last access: 1 March 2023.

Ferraccioli, F., Finn, C. A., Jordan, T. A., Bell, R. E., Anderson, L. M., and Damaske, D.: East Antarctic rifting triggers uplift of the Gamburtsev Mountains, Nature, 479, 388–392, https://doi.org/10.1038/nature10566, 2011.

Forsberg, R., Olesen, A. V., Ferraccioli, F., Jordan, T. A., Matsuoka, K., Zakrajsek, A., Ghidella, M., and Greenbaum, J. S.: Exploring the Recovery Lakes region and interior Dronning Maud Land, East Antarctica, with airborne gravity, magnetic and radar measurements, Geological Society, London, Special Publications, 461, 23, https://doi.org/10.1144/SP461.17, 2017.

Fox-Kemper, B., Hewitt, H. T., Xiao, C., Aðalgeirsdóttir, G., Drijfhout, S. S., Edwards, T. L., Golledge, N. R., Hemer, M., Kopp, R. E., Krinner, G., Mix, A., Notz, D., Nowicki, S., Nurhati, I. S., Ruiz, L., Sallée, J.-B., Slangen, A. B. A., and Yu, Y.: Ocean, Cryosphere and Sea Level Change, in: Climate Change 2021: The Physical Science Basis. Contribution of Working Group I to the Sixth Assessment Report of the Intergovernmental Panel on Climate Change, edited by: Masson-Delmotte, V., Zhai, P., Pirani, A., Connors, S. L., Péan, C., Berger, S., Caud, N., Chen, Y., Goldfarb, L., Gomis, M. I., Huang, M., Leitzell, K., Lonnoy, E., Matthews, J. B. R., Maycock, T. K., Waterfield, T., Yelekçi, O., Yu, R., and Zhou, B., Cambridge University Press, Cambridge, United Kingdom and New York, NY, USA, 1211–1362, https://doi.org/10.1017/9781009157896.011, 2021.

Frederick, B. C., Young, D. A., Blankenship, D. D., Richter, T. G., Kempf, S. D., Ferraccioli, F., and Siegert, M. J.: Distribution of subglacial sediments across the Wilkes Subglacial Basin, East Antarctica, J. Geophys. Res.-Earth, 121, 790–813, https://doi.org/10.1002/2015JF003760, 2016.

Fremand, A.: Polar Data Centre Geophysics book including Jupyter Notebooks for airborne geophysics and Bedmap projects – Snapshot (1.0), Zenodo [code], https://doi.org/10.5281/zenodo.7821671, 2023.

Frémand, A. C., Bodart, J. A., Jordan, T. A., Ferraccioli, F., Robinson, C., Corr, H. F. J., Peat, H. J., Bingham, R. G., and Vaughan, D. G.: British Antarctic Survey's aerogeophysical data: releasing 25 years of airborne gravity, magnetic, and radar datasets over Antarctica, Earth Syst. Sci. Data, 14, 3379–3410, https://doi.org/10.5194/essd-14-3379-2022, 2022a.

Fremand, A., Fretwell, P., Bodart, J., et al.: BEDMAP3 – Ice thickness, bed and surface elevation for Antarctica – standardised data points (Version 1.0), NERC EDS UK Polar Data Centre [data set], https://doi.org/jg6n, 2022b.

Fremand, A., Bodart, J., Fretwell, P., et al.: BEDMAP3 – Ice thickness, bed and surface elevation for Antarctica – standardised shapefiles and geopackages (Version 1.0), NERC EDS UK Polar Data Centre [data set], https://doi.org/jg8b, 2022c.

Fretwell, P., Pritchard, H. D., Vaughan, D. G., Bamber, J. L., Barrand, N. E., Bell, R., Bianchi, C., Bingham, R. G., Blankenship, D. D., Casassa, G., Catania, G., Callens, D., Conway, H., Cook, A. J., Corr, H. F. J., Damaske, D., Damm, V., Ferraccioli, F., Forsberg, R., Fujita, S., Gim, Y., Gogineni, P., Griggs, J. A., Hindmarsh, R. C. A., Holmlund, P., Holt, J. W., Jacobel, R. W., Jenkins, A., Jokat, W., Jordan, T., King, E. C., Kohler, J., Krabill, W., Riger-Kusk, M., Langley, K. A., Leitchenkov, G., Leuschen, C., Luyendyk, B. P., Matsuoka, K., Mouginot, J., Nitsche, F. O., Nogi, Y., Nost, O. A., Popov, S. V., Rignot, E., Rippin, D. M., Rivera, A., Roberts, J., Ross, N., Siegert, M. J., Smith, A. M., Steinhage, D., Studinger, M., Sun, B., Tinto, B. K., Welch, B. C., Wilson, D., Young, D. A., Xiangbin, C., and Zirizzotti, A.: Bedmap2: improved ice bed, surface and thickness datasets for Antarctica, The Cryosphere, 7, 375–393, https://doi.org/10.5194/tc-7-375-2013, 2013.

Fretwell, P., Fremand, A., Bodart, J., et al.: BEDMAP2 – Ice thickness, bed and surface elevation for Antarctica – standardised data points (Version 1.0), NERC EDS UK Polar Data Centre [data set], https://doi.org/jg6r, 2022a.

Fretwell, P., Pritchard, H., Vaughan, D., et al.: BEDMAP2 – Ice thickness, bed and surface elevation for Antarctica – standardised shapefiles and geopackages (Version 1.0), NERC EDS UK Polar Data Centre [data set], https://doi.org/jg6t, 2022b.

Fretwell, P., Pritchard, H. D., Vaughan, D. G., Bamber, J. L., Barrand, N. E., Bell, R., Bianchi, C., Bingham, R. G., Blankenship, D. D., Casassa, G., Catania, G., Callens, D., Conway, H., Cook, A. J., Corr, H. F. J., Damaske, D., Damm, V., Ferraccioli, F., Forsberg, R., Fujita, S., Gim, Y., Gogineni, P., Griggs, J. A., Hindmarsh, R. C. A., Holmlund, P., Holt, J. W., Jacobel, R. W., Jenkins, A., Jokat, W., Jordan, T., King, E. C., Kohler, J., Krabill, W., Riger-Kusk, M., Langley, K. A., Leitchenkov, G., Leuschen, C., Luyendyk, B. P., Matsuoka, K., Mouginot, J., Nitsche, F. O., Nogi, Y., Nost, O. A., Popov, S. V., Rignot, E., Rippin, D. M., Rivera, A., Roberts, J., Ross, N., Siegert, M. J., Smith, A. M., Steinhage, D., Studinger, M., Sun, B., Tinto, B. K., Welch, B. C., Wilson, D., Young, D. A., Xiangbin, C., and Zirizzotti, A.: BEDMAP2 – Ice thickness, bed and surface elevation for Antarctica – gridding products (Version 1.0), NERC EDS UK Polar Data Centre [data set], https://doi.org/jg6p, 2022c.

Gardner, A. S., Moholdt, G., Scambos, T., Fahnstock, M., Ligtenberg, S., van den Broeke, M., and Nilsson, J.: Increased West Antarctic and unchanged East Antarctic ice discharge over the last 7 years, The Cryosphere, 12, 521–547, https://doi.org/10.5194/tc-12-521-2018, 2018.

Gerrish, L., Ireland, L., Fretwell, P., and Cooper, P.: High resolution vector polygons of the Antarctic coastline (7.7), UK Polar Data Centre, Natural Environment Research Council, UK Research & Innovation [data set], https://doi.org/10.5285/0be5339c-9d35-44c9-a10f-da4b5356840b, 2023.

Global Change Master Directory (GCMD): GCMD Keywords, Version 15.9, Earth Science Data and Information System, Earth Science Projects Division, Goddard Space Flight Center (GSFC), National Aeronautics and Space Administration (NASA), https://forum.earthdata.nasa.gov/app.php/tag/GCMD+Keywords, last access: 29 May 2023.

Golledge, N. R., Kowalewski, D. E., Naish, T. R., Levy, R. H., Fogwill, C. J., and Gasson, E. G. W.: The multi-millennial Antarctic commitment to future sea-level rise, Nature, 526, 421–425, https://doi.org/10.1038/nature15706, 2015.

Hassell, D., Gregory, J., Blower, J., Lawrence, B. N., and Taylor, K. E.: A data model of the Climate and Forecast metadata conventions (CF-1.6) with a software implementation (cf-python v2.1), Geosci. Model Dev., 10, 4619–4646, https://doi.org/10.5194/gmd-10-4619-2017, 2017.

Holt, J. W., Blankenship, D. D., Morse, D. L., Young, D. A., Peters, M. E., Kempf, S. D., Richter, T. G., Vaughan, D. G., and Corr, H. F.: New boundary conditions for the West Antarctic Ice Sheet: Subglacial topography of the Thwaites and Smith glacier catchments, Geophys. Res. Lett., 33, L09502, https://doi.org/10.1029/2005GL025561, 2006.

IETF RFC 4180: Common Format and MIME Type for Comma-Separated Values (CSV) Files, https://www.ietf.org/rfc/rfc4180.txt (last access: 1 March 2023), 2005.

IRIS: GeoCSV: Tabular text formatting for geoscience data, http://geows.ds.iris.edu/documents/GeoCSV.pdf (last access: 29 May 2023), 2015.

Jordan, T. A., Martin, C., Ferraccioli, F., Matsuoka, K., Corr, H., Forsberg, R., Olesen, A., and Siegert, M.: Anomalously high geothermal flux near the South Pole, Sci. Rep., 8, 16785, https://doi.org/10.1038/s41598-018-35182-0, 2018.

Karlsson, N. B., Binder, T., Eagles, G., Helm, V., Pattyn, F., Van Liefferinge, B., and Eisen, O.: Glaciological characteristics in the Dome Fuji region and new assessment for "Oldest Ice", The Cryosphere, 12, 2413–2424, https://doi.org/10.5194/tc-12-2413-2018, 2018.

Levermann, A., Winkelmann, R., Albrecht, T., Goelzer, H., Golledge, N. R., Greve, R., Huybrechts, P., Jordan, J., Leguy, G., Martin, D., Morlighem, M., Pattyn, F., Pollard, D., Quiquet, A., Rodehacke, C., Seroussi, H., Sutter, J., Zhang, T., Van Breedam, J., Calov, R., DeConto, R., Dumas, C., Garbe, J., Gudmundsson, G. H., Hoffman, M. J., Humbert, A., Kleiner, T., Lipscomb, W. H., Meinshausen, M., Ng, E., Nowicki, S. M. J., Perego, M., Price, S. F., Saito, F., Schlegel, N.-J., Sun, S., and van de Wal, R. S. W.: Projecting Antarctica's contribution to future sea level rise from basal ice shelf melt using linear response functions of 16 ice sheet models (LARMIP-2), Earth Syst. Dynam., 11, 35–76, https://doi.org/10.5194/esd-11-35-2020, 2020.

Lythe, M. B. and Vaughan, D. G.: BEDMAP-bed topography of the Antarctic, British Antarctic Survey, Natural Environment Research Council, https://searchworks.stanford.edu/view/6750519 (last access: 29 May 2023), 2000.

Lythe, M. B. and Vaughan, D. G.: BEDMAP: A new ice thickness and subglacial topographic model of Antarc-

tica, J. Geophys. Res.-Sol. Ea., 106, 11335–11351, https://doi.org/10.1029/2000JB900449, 2001.

Lythe, M., Vaughan, D., BEDMAP 1, consortia, Fremand, A., and Bodart, J.: BEDMAP1 – Ice thickness, bed and surface elevation for Antarctica – standardised data points (Version 1.0), NERC EDS UK Polar Data Centre [data set], https://doi.org/jg6q, 2022a.

Lythe, M., Vaughan, D., BEDMAP 1, consortia, Fremand, A., and Bodart, J.: BEDMAP1 – Ice thickness, bed and surface elevation for Antarctica – standardised shapefiles and geopackages (Version 1.0), NERC EDS UK Polar Data Centre [data set], https://doi.org/jg6s, 2022b.

Lythe, M., Vaughan, D., and BEDMAP 1 Consortia: BEDMAP1 – Ice thickness, bed and surface elevation for Antarctica – gridding products (Version 1.0), NERC EDS UK Polar Data Centre [data set], https://doi.org/j2vz, 2023.

MacGregor, J. A., Boisvert, L. N., Medley, B., Petty, A. A., Harbeck, J. P., Bell, R. E., Blair, J. B., Blanchard-Wrigglesworth, E., Buckley, E. M., Christoffersen, M. S., Cochran, J. R., Csathó, B. M., De Marco, E. L., Dominguez, R. T., Fahnestock, M. A., Farrell, S. L., Gogineni, S. P., Greenbaum, J. S., Hansen, C. M., Hofton, M. A., Holt, J. W., Jezek, K. C., Koenig, L. S., Kurtz, N. T., Kwok, R., Larsen, C. F., Leuschen, C. J., Locke, C. D., Manizade, S. S., Martin, S., Neumann, T. A., Nowicki, S. M. J., Paden, J. D., Richter-Menge, J. A., Rignot, E. J., Rodríguez-Morales, F., Siegfried, M. R., Smith, B. E., Sonntag, J. G., Studinger, M., Tinto, K. J., Truffer, M., Wagner, T. P., Woods, J. E., Young, D. A., and Yungel, J. K.: The Scientific Legacy of NASA's Operation IceBridge, Rev. Geophys., 59, e2020RG000712, https://doi.org/10.1029/2020RG000712, 2021.

Morlighem, M., Rignot, E., Binder, T., Blankenship, D., Drews, R., Eagles, G., Eisen, O., Ferraccioli, F., Forsberg, R., Fretwell, P., Goel, V., Greenbaum, J. S., Gudmundsson, H., Guo, J., Helm, V., Hofstede, C., Howat, I., Humbert, A., Jokat, W., Karlsson, N. B., Lee, W. S., Matsuoka, K., Millan, R., Mouginot, J., Paden, J., Pattyn, F., Roberts, J., Rosier, S., Ruppel, A., Seroussi, H., Smith, E. C., Steinhage, D., Sun, B., Broeke, M. R. van den, Ommen, T. D. van, Wessem, M. van, and Young, D. A.: Deep glacial troughs and stabilizing ridges unveiled beneath the margins of the Antarctic ice sheet, Nat. Geosci., 13, 132–137, https://doi.org/10.1038/s41561-019-0510-8, 2020.

Mouginot, J., Rignot, E., and Scheuchl, B.: Sustained increase in ice discharge from the Amundsen Sea Embayment, West Antarctica, from 1973 to 2013, Geophys. Res. Lett., 41, 1576–1584, https://doi.org/10.1002/2013GL059069, 2014.

NCCSV: A NetCDF-Compatible ASCII CSV File Specification, https://coastwatch.pfeg.noaa.gov/erddap/download/NCCSV.html, last access: 1 March 2023.

Paxman, G. J. G., Jamieson, S. S. R., Ferraccioli, F., Jordan, T. A., Bentley, M. J., Ross, N., Forsberg, R., Matsuoka, K., Steinhage, D., Eagles, G., and Casal, T. G.: Subglacial Geology and Geomorphology of the Pensacola-Pole Basin, East Antarctica, Geochem. Geophy. Geosy., 20, 2786–2807, https://doi.org/10.1029/2018GC008126, 2019.

Pollard, D. and DeConto, R. M.: Modelling West Antarctic ice sheet growth and collapse through the past five million years, Nature, 458, 329–332, https://doi.org/10.1038/nature07809, 2009.

Popov, S.: Fifty-five years of Russian radio-echo sounding investigations in Antarctica, Ann. Glaciol., 61, 14–24, https://doi.org/10.1017/aog.2020.4, 2020.

Pritchard, H. D.: Bedgap: where next for Antarctic subglacial mapping?, Antarct. Science, 26, 742–757, https://doi.org/10.1017/S095410201400025X, 2014.

Rignot, E., Mouginot, J., Scheuchl, B., van den Broeke, M., van Wessem, M. J., and Morlighem, M.: Four decades of Antarctic Ice Sheet mass balance from 1979–2017, P. Natl. Acad. Sci. USA, 116, 1095–1103, https://doi.org/10.1073/pnas.1812883116, 2019.

Robin, G. D. Q., Swithinbank, C. W. M., and Smith, B. M. E.: Radio echo exploration of the Antarctic ice sheet, International Association of Scientific Hydrology Publication, 86, 97–115, 1970.

Scambos, T. A., Bell, R. E., Alley, R. B., Anandakrishnan, S., Bromwich, D. H., Brunt, K., Christianson, K., Creyts, T., Das, S. B., DeConto, R., Dutrieux, P., Fricker, H. A., Holland, D., MacGregor, J., Medley, B., Nicolas, J. P., Pollard, D., Siegfried, M. R., Smith, A. M., Steig, E. J., Trusel, L. D., Vaughan, D. G., and Yager, P. L.: How much, how fast?: A science review and outlook for research on the instability of Antarctica's Thwaites Glacier in the 21st century, Global Planet. Change, 153, 16–34, https://doi.org/10.1016/j.gloplacha.2017.04.008, 2017.

Schroeder, D. M., Dowdeswell, J. A., Siegert, M. J., Bingham, R. G., Chu, W., MacKie, E. J., Siegfried, M. R., Vega, K. I., Emmons, J. R., and Winstein, K.: Multidecadal observations of the Antarctic ice sheet from restored analog radar records, P. Natl. Acad. Sci. USA, 116, 18867–18873, https://doi.org/10.1073/pnas.1821646116, 2019.

Schroeder, D. M., Bingham, R. G., Blankenship, D. D., Christianson, K., Eisen, O., Flowers, G. E., Karlsson, N. B., Koutnik, M. R., Paden, J. D., and Siegert, M. J.: Five decades of radioglaciology, Ann. Glaciol., 61, 1–13, https://doi.org/10.1017/aog.2020.11, 2020.

Schroeder, D. M., Broome, A. L., Conger, A., Lynch, A., Mackie, E. J., and Tarzona, A.: Radiometric analysis of digitized Z-scope records in archival radar sounding film, J. Glaciol., 68, 733–740, https://doi.org/10.1017/jog.2021.130, 2021.

Seroussi, H., Nowicki, S., Payne, A. J., Goelzer, H., Lipscomb, W. H., Abe-Ouchi, A., Agosta, C., Albrecht, T., Asay-Davis, X., Barthel, A., Calov, R., Cullather, R., Dumas, C., Galton-Fenzi, B. K., Gladstone, R., Golledge, N. R., Gregory, J. M., Greve, R., Hattermann, T., Hoffman, M. J., Humbert, A., Huybrechts, P., Jourdain, N. C., Kleiner, T., Larour, E., Leguy, G. R., Lowry, D. P., Little, C. M., Morlighem, M., Pattyn, F., Pelle, T., Price, S. F., Quiquet, A., Reese, R., Schlegel, N.-J., Shepherd, A., Simon, E., Smith, R. S., Straneo, F., Sun, S., Trusel, L. D., Van Breedam, J., van de Wal, R. S. W., Winkelmann, R., Zhao, C., Zhang, T., and Zwinger, T.: ISMIP6 Antarctica: a multi-model ensemble of the Antarctic ice sheet evolution over the 21st century, The Cryosphere, 14, 3033–3070, https://doi.org/10.5194/tc-14-3033-2020, 2020.

Shepherd, A., Ivins, E. R., A, G., Barletta, V. R., Bentley, M. J., Bettadpur, S., Briggs, K. H., Bromwich, D. H., Forsberg, R., Galin, N., Horwath, M., Jacobs, S., Joughin, I., King, M. A., Lenaerts, J. T. M., Li, J., Ligtenberg, S. R. M., Luckman, A., Luthcke, S. B., McMillan, M., Meister, R., Milne, G., Mouginot, J., Muir, A., Nicolas, J. P., Paden, J., Payne, A. J., Pritchard, H., Rignot, E., Rott, H., Sørensen, L. S., Scambos, T. A., Scheuchl,

B., Schrama, E. J. O., Smith, B., Sundal, A. V., van Angelen, J. H., van de Berg, W. J., van den Broeke, M. R., Vaughan, D. G., Velicogna, I., Wahr, J., Whitehouse, P. L., Wingham, D. J., Yi, D., Young, D., and Zwally, H. J.: A Reconciled Estimate of Ice-Sheet Mass Balance, Science, 338, 1183–1189, https://doi.org/10.1126/science.1228102, 2012.

Sun, B., Siegert, M. J., Mudd, S. M., Sugden, D., Fujita, S., Xiangbin, C., Yunyun, J., Xueyuan, T., and Yuansheng, L.: The Gamburtsev mountains and the origin and early evolution of the Antarctic Ice Sheet, Nature, 459, 690–693, https://doi.org/10.1038/nature08024, 2009.

The IMBIE team: Mass balance of the Antarctic Ice Sheet from 1992 to 2017, Nature, 558, 219–222, https://doi.org/10.1038/s41586-018-0179-y, 2018.

Turchetti, S., Dean, K., Naylor, S., and Siegert, M.: Accidents and Opportunities: A History of the Radio Echo Sounding (RES) of Antarctica, 1958–1979, British Journal of the History of Science, 41, 417–444, https://doi.org/10.1017/S0007087408000903, 2008.

UK Government: Tabular data standard, https://www.gov.uk/government/publications/recommended-open-standards-for-government/tabular-data-standard (last access: 1 March 2023), 2020.

UK Polar Data Centre: Geophysics book, https://antarctica.github.io/PDC_GeophysicsBook, last access: 1 March 2023a.

UK Polar Data Centre: Geophysics book, UK Polar Data Centre, https://antarctica.github.io/PDC_GeophysicsBook/BEDMAP/Downloading_the_Bedmap_data.html, last access: 1 March 2023b.

Vaughan, D. G., Corr, H. F., Ferraccioli, F., Frearson, N., O'Hare, A., Mach, D., Holt, J. W., Blankenship, D. D., Morse, D. L., and Young, D. A.: New boundary conditions for the West Antarctic ice sheet: Subglacial topography beneath Pine Island Glacier, Geophys. Res. Lett., 33, L09501, https://doi.org/10.1029/2005GL025588, 2006.

Wilkinson, M. D., Dumontier, M., Aalbersberg, Ij. J., Appleton, G., Axton, M., Baak, A., Blomberg, N., Boiten, J.-W., da Silva Santos, L. B., Bourne, P. E., Bouwman, J., Brookes, A. J., Clark, T., Crosas, M., Dillo, I., Dumon, O., Edmunds, S., Evelo, C. T., Finkers, R., Gonzalez-Beltran, A., Gray, A. J. G., Groth, P., Goble, C., Grethe, J. S., Heringa, J., 't Hoen, P. A. C., Hooft, R., Kuhn, T., Kok, R., Kok, J., Lusher, S. J., Martone, M. E., Mons, A., Packer, A. L., Persson, B., Rocca-Serra, P., Roos, M., van Schaik, R., Sansone, S.-A., Schultes, E., Sengstag, T., Slater, T., Strawn, G., Swertz, M. A., Thompson, M., van der Lei, J., van Mulligen, E., Velterop, J., Waagmeester, A., Wittenburg, P., Wolstencroft, K., Zhao, J., and Mons, B.: The FAIR Guiding Principles for scientific data management and stewardship, Sci. Data, 3, 160018, https://doi.org/10.1038/sdata.2016.18, 2016.

Table S1. List of survey data used to build Bedmap2. For each survey we provide the project name, institution, reference, source (DOI), firn correction, history, electromagnetic wave speed in ice, instrument used for acquisition and the centre frequency.

filename	project	institution	reference	source	firn cor-rection	history	electromag netic wave speed in ice	instrument	centre frequency
AWI_1994_DML1_AIR_BM2	Dronning Maud Land	Alfred Wegener Institute	https://doi.org/10.3189/172756499781820996	https://doi.org/10.1594/PANGAEA.957053	0	Incoherent	168.1	AWI EMR	150
AWI_1995_DML2_AIR_BM2	Dronning Maud Land	Alfred Wegener Institute	https://hdl.handle.net/10013/epic.15056	https://doi.org/10.1594/PANGAEA.957054	0	Incoherent	168.1	AWI EMR	150
AWI_1996_DML3_AIR_BM2	Dronning Maud Land	Alfred Wegener Institute	https://hdl.handle.net/10013/epic.15056	https://doi.org/10.1594/PANGAEA.957056	0	Incoherent	168.1	AWI EMR	150
AWI_1997_DML4_AIR_BM2	Dronning Maud Land	Alfred Wegener Institute	https://hdl.handle.net/10013/epic.15056	https://doi.org/10.1594/PANGAEA.957058	0	Incoherent	168.1	AWI EMR	150
AWI_1998_DML5_AIR_BM2	Dronning Maud Land	Alfred Wegener Institute	https://hdl.handle.net/10013/epic.15056	https://doi.org/10.1594/PANGAEA.957059	0	Incoherent	168.1	AWI EMR	150
AWI_2000_DML6_AIR_BM2	Dronning Maud Land	Alfred Wegener Institute	https://doi.org/10.1111/j.1365-246X.2012.05363.x	https://doi.org/10.1594/PANGAEA.957061	0	Incoherent	168.1	AWI EMR	150
AWI_2001_DML7_AIR_BM2	Dronning Maud Land	Alfred Wegener Institute	https://doi.org/10.1111/j.1365-246X.2012.05363.x	https://doi.org/10.1594/PANGAEA.957063	0	Incoherent	168.1	AWI EMR	150
AWI_2002_DML8_AIR_BM2	Dronning Maud Land	Alfred Wegener Institute	https://doi.org/10.1111/j.1365-246X.2012.05363.x	https://doi.org/10.1594/PANGAEA.957062	0	Incoherent	168.1	AWI EMR	150
AWI_2003_DML9_AIR_BM2	Dronning Maud Land	Alfred Wegener Institute	https://doi.org/10.1111/j.1365-246X.2012.05363.x	https://doi.org/10.1594/PANGAEA.957064	0	Incoherent	168.1	AWI EMR	150
AWI_2004_DML10_AIR_BM2	Dronning Maud Land	Alfred Wegener Institute	https://doi.org/10.1111/j.1365-246X.2012.05363.x	https://doi.org/10.1594/PANGAEA.957060	0	Incoherent	168.1	AWI EMR	150
AWI_2005_ANTSYSO_AIR_BM2	Shirase Glacier; Syowa Station; Dronning Maud Land (ANTSYSO)	Alfred Wegener Institute; National Institute of Polar Research	https://doi.org/10.1016/j.precamres.2013.02.008	https://doi.org/10.1594/PANGAEA.957065	0	Incoherent	168.1	AWI EMR	150
AWI_2007_ANTR_AIR_BM2	Dronning Maud Land; Princess Elizabeth Land; Dome A; Dome C	Alfred Wegener Institute	https://doi.org/10.5194/essd-11-1069-2019	https://doi.org/10.1594/PANGAEA.957066	0	Incoherent	168.1	AWI EMR	150
BAS_1994_Evans_AIR_BM2	Evans Ice Stream	British Antarctic Survey	https://doi.org/10.1016/S0040-1951(01)00236-0	https://doi.org/10.5285/2C261013-9A0E-447D-A5BB-B506610B14FF	10	Incoherent	168	BAS-built	150
BAS_1998_Dufek_AIR_BM2	Dufek Massif	British Antarctic Survey	https://doi.org/10.1016/S0012-821X(97)00165-9	https://doi.org/10.5285/5E2CF315-9265-4605-8643-382F2557009B	10	Incoherent	168	BAS-built	150
BAS_2001_Bailey-Slessor_AIR_BM2	Bailey Ice Stream; Slessor Glacier	British Antarctic Survey	https://doi.org/10.1029/2003JF000039	https://doi.org/10.5285/C5175014-A056-4799-A8C0-65B5FC433743	10	Incoherent	168	BAS-built	150

BAS_2001_MAMOG_AIR_BM2	Jutulstraumen Ice Stream (MAMOG)	British Antarctic Survey	https://doi.org/10.1111/j.1365-3121.2005.00651.x	https://doi.org/10.5285/84A273D9-8191-4316-B8F6-DC907EB0947A	10	Incoherent	168	BAS-built	150
BAS_2001_TORUS_AIR_BM2	Rutford Ice Stream (TORUS)	British Antarctic Survey	https://doi.org/10.5194/essd-14-3379-2022	https://doi.org/10.5285/4B2CCDA1-91EC-4C57-9AE0-07B9A387F352	10	Incoherent	168	BAS-built	150
BAS_2004_BBAS_AIR_BM2	Pine Island Glacier (BBAS)	British Antarctic Survey	https://doi.org/10.1029/2005GL025588	https://doi.org/10.5285/3ADB739A-9EDA-434D-9883-03AB092CABAE	10	Incoherent	168	PASIN	150
BAS_2005_WISE-ISODYN_AIR_BM2	Wilkes Subglacial Basin (WISE-ISODYN)	British Antarctic Survey	https://doi.org/10.5194/essd-14-3379-2022	https://doi.org/10.5285/59e5a6f5-e67d-4a05-99af-30f656569401	10	2D Synthetic Aperture Radar	168	PASIN	150
BAS_2006_GRADES-IMAGE_AIR_BM2	Evans Ice Stream; Rutford Ice Stream (GRADES-IMAGE)	British Antarctic Survey	https://doi.org/10.3189/2014AoG67A052	https://doi.org/10.5285/4EFA688E-7659-4CBF-A72F-FACAC5D63998	10	2D Synthetic Aperture Radar	168	PASIN	150
BAS_2007_AGAP_AIR_BM2	Gamburtsev Subglacial Mountains; Dome A (AGAP)	British Antarctic Survey	https://doi.org/10.1038/nature10566	https://doi.org/10.5285/0f6f5a45-d8af-4511-a264-b0b35ee34af6	10	2D Synthetic Aperture Radar	168	PASIN	150
BAS_2007_TIGRIS_GRN_BM2	Pine Island Glacier (TIGRIS)	British Antarctic Survey; University of Edinburgh	https://doi.org/10.1038/s41467-017-01597-y	-9999	10	2-D migration	168	DELORES	2
BAS_2009_Ferrigno_GRN_BM2	Ferrigno Ice Stream	British Antarctic Survey; University of Edinburgh	https://doi.org/10.1038/nature11292	-9999	10	2-D migration	168.5	DELORES	2
BAS_2010_IMAFI_AIR_BM2	Institute-Möller Ice Stream (IMAFI)	British Antarctic Survey	https://doi.org/10.1038/NGEO1468	https://doi.org/10.5285/7946C497-72FC-41CB-A9B2-BF9980EFE156	10	2D Synthetic Aperture Radar	168	PASIN	150
BAS_2010_PIG_AIR_BM2	Pine Island Glacier Ice Shelf	British Antarctic Survey	https://doi.org/10.1029/2012JF002360	https://doi.org/10.5285/E88F651C-3389-4D99-8333-07872DCEAB57	10	2D Synthetic Aperture Radar	168	PASIN	150
BGR_1999_GANOVEX-VIII-Mertz_AIR_BM2	Mertz Glacier (GANOVEX VIII)	Bundesanstalt für Geowissenschaften und Rohstoffe	-9999	-9999	0	Linear/logarithmic signal detection	168	BGR-TUHH helicopter-borne	150
BGR_1999_GANOVEX-VIII-Matusevich_AIR_BM2	Matusevich Glacier (GANOVEX VIII)	Bundesanstalt für Geowissenschaften und Rohstoffe	-9999	-9999	0	Linear/logarithmic signal detection	168	BGR-TUHH helicopter-borne	150
BGR_2002_PCMEGA_AIR_BM2	Lambert Glacier; Prince Charles Mountains (PCMEGA)	Bundesanstalt für Geowissenschaften und Rohstoffe	https://doi.org/10.1007/s00190-007-0189-2	-9999	0	Logarithmic signal detection	168	BGR-TUHH fixed-wing aircraft	150
INGV_1997_ITASE_AIR_BM2	Talos Dome; Oats Land (ITASE)	Istituto Nazionale di Geofisica e Vulcanologia	https://doi.org/10.3189/172756404781814591	-9999	-9999	-9999	168	INGV-IT GlacioRadar	60
LDEO_2007_Recovery-Lakes_AIR_BM2	Recovery Lakes	Lamont-Doherty Earth Observatory	-9999	-9999	-9999	1-D Synthetic Aperture Radar	-9999	LDEO radar	150

LDEO_2007_AGAP-GAMBIT_AIR_BM2	Gamburtsev Subglacial Mountains; Dome A (AGAP)	Lamont-Doherty Earth Observatory	https://doi.org/10.1126/science.1200109	https://doi.org/10.1594/IEDA/317765	-9999	1-D Synthetic Aperture Radar	-9999	LDEO radar	150
NASA_2002_ICEBRIDGE_AIR_BM2	NASA Operation IceBridge	Center for Remote Sensing of Ice Sheets; National Aeronautics and Space Administration; Centro de Estudios Científicos	https://doi.org/10.3189/172756404781813916	https://data.cresis.ku.edu/	0	2-D Synthetic Aperture Radar focused	169	ICORDS2	150
NASA_2004_ICEBRIDGE_AIR_BM2	NASA Operation IceBridge	Center for Remote Sensing of Ice Sheets	-9999	https://data.cresis.ku.edu/	0	2-D Synthetic Aperture Radar focused	169	ACORDS	150
NASA_2009_ICEBRIDGE_AIR_BM2	NASA Operation IceBridge	Center for Remote Sensing of Ice Sheets	https://doi.org/10.1029/2020RG000712	https://data.cresis.ku.edu/	0	2-D Synthetic Aperture Radar focused	169	MCoRDS	189-201
NASA_2010_ICEBRIDGE_AIR_BM2	NASA Operation IceBridge	Center for Remote Sensing of Ice Sheets	https://doi.org/10.1029/2020RG000712	https://data.cresis.ku.edu/	0	2-D Synthetic Aperture Radar focused	169	MCoRDS	189-199
NASA_2011_ICEBRIDGE_AIR_BM2	NASA Operation IceBridge	Center for Remote Sensing of Ice Sheets	https://doi.org/10.1029/2020RG000712	https://data.cresis.ku.edu/	0	2-D Synthetic Aperture Radar focused	169	MCoRDS	189-200
NASA_2012_ICEBRIDGE_AIR_BM2	NASA Operation IceBridge	Center for Remote Sensing of Ice Sheets	https://doi.org/10.1029/2020RG000712	https://data.cresis.ku.edu/	0	2-D Synthetic Aperture Radar focused	169	MCoRDS	189-200
NIPR_1999_JARE40_GRN_BM2	Dome Fuji (JARE40)	Japanese Antarctic Research Expedition; National Institute of Polar Research	-9999	-9999	-9999	Incoherent	168.7	VHF179	179
NIPR_2007_JASE_GRN_BM2	Dome Fuji (JASE)	Japanese Antarctic Research Expedition; National Institute of Polar Research	-9999	-9999	-9999	Incoherent	168.7	VHF179	179
NIPR_2007_JARE49_GRN_BM2	Dome Fuji (JARE-49)	Japanese Antarctic Research Expedition; National Institute of Polar Research	-9999	-9999	-9999	Coherent; Incoherent	168.7	POL179	179
NPI_2008_BELISSIMA_GRN_BM2	Roi Baudoin Ice Shelf Ice Rise	Norwegian Polar Institute	https://doi.org/10.3189/2012AoG60A106	-9999	0	Incoherent	168.4	University of Washington radar	5
NPI_2010_SRM_AIR_BM2	Sør Rondane Mountains; Dronning Maud Land	Norwegian Polar Institute	https://doi.org/10.3189/2015AoG70A010	https://doi.org/10.1594/PANGAEA.836299	0	Incoherent	168	AWIRES	150
PRIC_2007_CHINARE-24_GRN_BM2	Dome A (CHINARE-24)	Polar Research Institute of China	https://doi.org/10.1007/s11434-009-0546-z	-9999	0	Incoherent	168	NIPR radar	179
PRIC_2004_CHINARE-21_GRN_BM2	Dome A; Zhongshan Station (CHINARE-21)	Polar Research Institute of China	https://doi.org/10.1007/s11434-010-3238-9	-9999	0	Incoherent	168	NIPR radar	179
RNRF_2003_48RAEap5_AIR_BM2	Princess Elizabeth Land	Polar Marine Geosurvey Expedition	https://doi.org/10.1017/aog.2020.4	-9999	0	Incoherent	168	MPI-60	60
RNRF_2004_49RAEap5_AIR_BM2	Princess Elizabeth Land	Polar Marine Geosurvey Expedition	https://doi.org/10.1017/aog.2020.4	-9999	0	Incoherent	168	MPI-60	60
RNRF_2005_50RAEap5_AIR_BM2	Princess Elizabeth Land	Polar Marine Geosurvey Expedition	https://doi.org/10.1017/aog.2020.4	-9999	0	Incoherent	168	MPI-60	60

RNRF_2006_51RAEap5_AIR_BM2	Princess Elizabeth Land	Polar Marine Geosurvey Expedition	https://doi.org/10.1017/aog.2020.4	-9999	0	Incoherent	168	MPI-60	60
RNRF_2006_KV1-area_AIR_BM2	Princess Elizabeth Land	Polar Marine Geosurvey Expedition	https://doi.org/10.1017/aog.2020.4	-9999	0	Incoherent	168	RLS-60-98	60
RNRF_2007_52RAEap5_AIR_BM2	Princess Elizabeth Land	Polar Marine Geosurvey Expedition	https://doi.org/10.1017/aog.2020.4	-9999	0	Incoherent	168	MPI-60	60
RNRF_2007_Mirny-Vostok_AIR_BM2	Mirny Station; Vostok traverse	Polar Marine Geosurvey Expedition	https://doi.org/10.1017/aog.2020.4	-9999	0	Incoherent	168	RLS-60-98	60
RNRF_2008_Vostok-Subglacial-Lake_AIR_BM2	Vostok Subglacial Lake	Polar Marine Geosurvey Expedition	https://doi.org/10.15356/2076-6734-2012-4-31-38	-9999	0	Incoherent	168.4	RLS-60-98	60
RNRF_2008_53RAEap5_AIR_BM2	Princess Elizabeth Land	Polar Marine Geosurvey Expedition	https://doi.org/10.1017/aog.2020.4	-9999	0	Incoherent	168	MPI-60	60
RNRF_2013_Vostok-Progress_AIR_BM2	Vostok Station; Progress Station traverse	Polar Marine Geosurvey Expedition	https://doi.org/10.1017/aog.2020.4	-9999	0	Incoherent	168	RLS-60-06	60
STOLAF_1994_Siple-Dome_GRN_BM2	Siple Dome	St. Olaf College	https://doi.org/10.1029/95JB03735	https://doi.org/10.7265/N5Z31WJQ	0	2-D migration	168.5	St. Olaf College radar	3-5
STOLAF_2001_ITASE-Byrd-Ellsworth_GRN_BM2	Byrd Ice Core; Ellsworth Mountains (US-ITASE)	St. Olaf College	https://doi.org/10.1029/2003GL017210	https://doi.org/10.7265/N5R20Z9T	0	2-D migration	168.5	St. Olaf College radar	3
STOLAF_2001_ITASE-Ellsworth_GRN_BM2	Ellsworth Mountains (US-ITASE)	St. Olaf College	https://doi.org/10.1029/2003GL017210	https://doi.org/10.7265/N5R20Z9T	0	2-D migration	168.5	St. Olaf College radar	3
STOLAF_2002_ITASE-Hercules-Dome_GRN_BM2	Hercules Dome (US-ITASE)	St. Olaf College	https://doi.org/10.1029/2004JF000188	https://doi.org/10.7265/N5R20Z9T	0	2-D migration	168.5	St. Olaf College radar	3
STOLAF_2002_ITASE-Byrd-South-Pole_GRN_BM2	Byrd Ice core; South Pole (US-ITASE)	St. Olaf College	https://doi.org/10.1029/2004JF000188	https://doi.org/10.7265/N5R20Z9T	0	2-D migration	168.5	St. Olaf College radar	3
UCANTERBURY_2008_Darwin-Hatherton_GRN_BM2	Darwin–Hatherton glacial system	Gateway Antarctica University of Canterbury	https://doi.org/10.1017/jog.2017.60	-9999	4.7	Migration	168	pulseEKKO PRO	25
UTIG_1991_CASERTZ_AIR_BM2	Byrd Subglacial Basin; Bindschadler Ice Stream; Kamb Ice Stream; Willians Ice Stream	University of Texas Institute for Geophysics	https://doi.org/10.1029/AR077p0105	https://doi.org/10.15784/601588	0	Incoherent log-dectected	168.37	SOAR TUD IV (RADsh1, RADgh1 digitizer)	60
UTIG_1998_West-Marie-Byrd-Land_AIR_BM2	Western Marie Byrd Land	University of Texas Institute for Geophysics	https://doi.org/10.1029/2002GC000462	https://doi.org/10.7265/N5BZ63ZH	0	Incoherent log-dectected	168.37	SOAR TUD IV (RADgh1 digitizer)	60
UTIG_1999_SOAR-LVS-WLK_AIR_BM2	Transantarctic Mountains; South Pole; Lake Vostok; Dome C	University of Texas Institute for Geophysics; Lamont-Doherty Earth Observatory	http://dx.doi.org/10.1016/S0012-821X(04)00066-4	https://doi.org/10.15784/601588	0	Incoherent log-dectected	168.37	SOAR TUD IV (RADgh1 digitizer)	60
UTIG_2000_Robb-Glacier_AIR_BM2	Robb Glacier	University of Texas Institute for Geophysics	-9999	https://doi.org/10.15784/601604	0	Incoherent log-dectected	168.37	SOAR TUD IV (RADgh1 digitizer)	60

UTIG_2004_AGASEA_AIR_BM2	Thwaites Glacier; Smith Glacier (AGASEA)	University of Texas Institute for Geophysics	https://doi.org/10.1029/2005GL025561	https://doi.org/10.7265/N5W95730	0	2-D Synthetic Aperture Radar focused	168.4	HICARS	60
UTIG_2008_ICECAP_AIR_BM2	Aurora Subglacial Basin	University of Texas Institute for Geophysics	http://dx.doi.org/10.1038/nature10114	https://doi.org/10.5067/F5FGUT9F5089	0	pik1 (short coherent)	168.4	HICARS	60

Table S2. List of survey data added as part of the Bedmap3 release. . For each survey we provide the project name, institution, reference, source (DOI), firn correction, history, electromagnetic wave speed in ice, instrument used for acquisition and the centre frequency.

filename	project	institution	reference	source	firn correction	history	electromagnetic wave speed in ice	instrument	centre frequency
AWI_2013_GEA-IV_AIR_BM3	Dronning Maud Land (GEA-IV)	Alfred Wegener Institute; Bundesanstalt für Geowissenschaften	https://doi.org/10.1016/j.gr.2018.05.011	https://doi.org/10.1594/PANGAEA.938357	10	Incoherent	167.0	AWI EMR	150
AWI_2014_Recovery-Glacier_AIR_BM3	Recovery Glacier	Alfred Wegener Institute	https://doi.org/10.1029/2017JF004591	https://doi.org/10.1594/PANGAEA.894292	0	Incoherent	168.1	AWI EMR	150
AWI_2015_GEA-DML_AIR_BM3	Dronning Maud Land (GEA)	Alfred Wegener Institute; Bundesanstalt für Geowissenschaften	https://doi.org/10.1016/j.gr.2018.05.011	https://doi.pangaea.de/10.1594/PANGAEA.915475	0	Incoherent	168.0	AWI EMR	150
AWI_2016_OIR_AIR_BM3	Dome Fuji (Oldest Ice Reconnaissance)	Alfred Wegener Institute	https://doi.org/10.5194/tc-12-2413-2018	https://doi.pangaea.de/10.1594/PANGAEA.891323	10	Incoherent	167.0	AWI EMR	150
AWI_2018_DML-Coast_AIR_BM3	Dronning Maud Land coast	Alfred Wegener Institute; Tübingen University	-9999	https://doi.pangaea.de/10.1594/PANGAEA.911868	0	2D Synthetic Aperture Radar focussed	168.9	AWI UWB (MCoRDS v5)	195
AWI_2018_ANIRES_AIR_BM3	Dronning Maud Land (AniRES)	Tübingen University; Alfred Wegener Institute	-9999	-9999	8	Incoherent	168.0	AWI EMR	150
AWI_2018_JURAS_AIR_BM3	Jutulstraumen Ice Stream (JURAS)	Alfred Wegener Institute	https://doi.org/10.1002/esp.5203	https://doi.org/10.1594/PANGAEA.911475	0	2D Synthetic Aperture Radar focussed	168.9	AWI UWB (MCoRDS v5)	195
AWI_2019_JURAS_AIR_BM3	Jutulstraumen Ice Stream (JURAS)	Alfred Wegener Institute	-9999	https://doi.pangaea.de/10.1594/PANGAEA.910019	0	2D Synthetic Aperture Radar focussed	168.9	AWI UWB (MCoRDS v5)	195
BAS_2007_Lake-Ellsworth_GRN_BM3	Lake Ellsworth	British Antarctic Survey; Newcastle University	https://doi.org/10.1017/aog.2020.50	-9999	0	2-D migration	168	DELORES	2
BAS_2007_Rutford_GRN_BM3	Rutford Ice Stream	British Antarctic Survey	https://doi.org/10.5194/essd-8-151-2016	https://dx.doi.org/10.5285/54757cbe-0b13-4385-8b31-4dfaa1dab55e	10	2-D migration	167	DELORES	3
BAS_2008_Lake-Ellsworth_GRN_BM3	Lake Ellsworth	British Antarctic Survey; Newcastle University	https://doi.org/10.1017/aog.2020.50	-9999	0	2-D migration	168	DELORES	2
BAS_2010_IMAFI_AIR_BM3	Institute-Möller Ice Stream (IMAFI)	British Antarctic Survey	https://doi.org/10.1038/ngeo1468	https://doi.org/10.5285/7946c497-72fc-41cb-a9b2-bf9980efe156	10	2-D Synthetic Aperture Radar	168	PASIN	150
BAS_2011_Adelaide_AIR_BM3	Adelaide Island	British Antarctic Survey	https://doi.org/10.1093/gji/ggu233	-9999	10	2-D Synthetic Aperture Radar	168	PASIN	150
BAS_2012_Castle_GRN_BM3	Pine Island Glacier	British Antarctic Survey	-9999	-9999	10	2-D Synthetic Aperture Radar	168	DELORES	2

BAS_2012_ICEGRAV_AIR_BM3	Recovery Catchment (ICEGRAV)	British Antarctic Survey	https://doi.org/10.1144/SP461.17	https://doi.org/10.5285/6549203d-da8b-4a22-924b-a9e1471ea7f1	10	2-D Synthetic Aperture Radar	168	PASIN	150
BAS_2013_ISTAR_GRN_BM3	Pine Island Glacier (iSTAR)	British Antarctic Survey; University of Edinburgh	https://doi.org/10.1038/s41467-017-01597-y	-9999	10	2-D migration	168	DELORES	2
BAS_2015_POLARGAP_AIR_BM3	South Pole (PolarGAP)	British Antarctic Survey; European Space Agency	https://doi.org/10.1038/s41598-018-35182-0	https://doi.org/10.5270/esa-8ffoo3e	10	2-D Synthetic Aperture Radar	168	PASIN	150
BAS_2015_FISS_AIR_BM3	Filchner Ice Shelf System (FISS)	British Antarctic Survey	https://doi.org/10.5194/tc-15-1517-2021	https://doi.org/10.5285/144ceb0d-9d76-4a39-aa01-7b94ac80fac9	10	2-D Synthetic Aperture Radar	168	PASIN	150
BAS_2016_FISS_AIR_BM3	Filchner Ice Shelf System (FISS)	British Antarctic Survey	https://doi.org/10.5194/essd-14-3379-2022	https://doi.org/10.5285/e7851bba-21ff-4645-b557-d8eafdf89462	10	2-D Synthetic Aperture Radar	168	PASIN	150
BAS_2017_English-Coast_AIR_BM3	English Coast	British Antarctic Survey	https://doi.org/10.5194/essd-14-3379-2022	https://doi.org/10.5285/e07d62bf-d58c-4187-a019-59be998939cc	10	2-D Synthetic Aperture Radar	168	PASIN	150
BAS_2018_Thwaites_AIR_BM3	Thwaites Glacier (ITGC)	British Antarctic Survey	https://doi.org/10.5194/tc-14-2869-2020	https://data.cresis.ku.edu/	10	2-D Synthetic Aperture Radar	168	PASIN	150
BAS_2019_Thwaites_AIR_BM3	Thwaites Glacier (ITGC)	British Antarctic Survey	https://doi.org/10.5194/essd-14-3379-2022	https://doi.org/10.5285/7c12898d-7e55-458c-ba7d-ecec8252f3b5	10	2-D Synthetic Aperture Radar	168	PASIN	150
CRESIS_2009_Thwaites_AIR_BM3	Thwaites Glacier	Center for Remote Sensing of Ice Sheets	https://doi.org/10.1130/g46772.1	http://hdl.handle.net/1773/44950	0	MUSIC (Swath) Processing	168.91	MCoRDS	150
CRESIS_2009_Antarctica-TO_AIR_BM3	Thwaites Glacier; Pine Island Glacier	Center for Remote Sensing of Ice Sheets	https://doi.org/10.1130/g46772.1	https://doi.org/10.7910/DVN/M4C540	0	Synthetic Aperture Radar focused	168.91	MCoRDS	150
CRESIS_2013_Siple-Coast_AIR_BM3	Siple Coast	Center for Remote Sensing of Ice Sheets	https://doi.org/10.1109/JSTARS.2015.2403611	https://data.cresis.ku.edu/	0	Synthetic Aperture Radar focused	168.91	MCoRDS v4	150-450
CECS_2006_Subglacial-Lake-CECs_GRN_BM3	Subglacial Lake Centro de Estudios Científicos	Centro de Estudios Científicos	https://doi.org/10.1002/2015GL063390	-9999	-9999	Synthetic Aperture Radar unfocused	168	CECS radar	155
INGV_1997_Talos-Dome_AIR_BM3	Talos Dome; Terre Adelie	Istituto Nazionale di Geofisica e Vulcanologia	https://doi.org/10.4401/ag-3471	-9999	-9999	-9999	168	INGV-IT GlacioRadar	60
INGV_1999_Talos-Dome_AIR_BM3	Talos Dome; Terre Adelie	Istituto Nazionale di Geofisica e Vulcanologia	https://doi.org/10.4401/ag-3471	-9999	-9999	-9999	168	INGV-IT GlacioRadar	60
INGV_2001_Talos-Dome_AIR_BM3	Talos Dome; Oats Land	Istituto Nazionale di Geofisica e Vulcanologia	-9999	-9999	-9999	-9999	168	INGV-IT GlacioRadar	150
INGV_2003_Talos-Dome_AIR_BM3	Talos Dome; Queen Mary Land; Terre Adelie	Istituto Nazionale di Geofisica e Vulcanologia	-9999	-9999	-9999	-9999	168	INGV-IT GlacioRadar	60

LDEO_2015_ROSETTA_AIR_BM3	Ross Ice Shelf (ROSETTA)	Lamont-Doherty Earth Observatory	https://doi.org/10.1029/2019JF005241	http://www.ldeo.columbia.edu/polar-geophysics-group/data	0	1-D Synthetic Aperture Radar	168	DICE IcePod	188
NIPR_1992_JARE33_GRN_BM3	Dome Fuji (JARE33)	Japanese Antarctic Research Expedition; National Institute of Polar Research	https://doi.org/10.1029/1999JB900034	https://doi.org/10.17592/001.2021110902	-9999	Incoherent	168.7	VHF179	179
NIPR_1996_JARE37_GRN_BM3	Dome Fuji (JARE37)	Japanese Antarctic Research Expedition; National Institute of Polar Research	https://doi.org/10.1029/1999JB900034	https://doi.org/10.17592/001.2021110903 https://doi.org/10.17592/001.2022072001	-9999	Incoherent	168.7	VHF179	179
NIPR_1999_JARE40_GRN_BM3	Dome Fuji (JARE40)	Japanese Antarctic Research Expedition; National Institute of Polar Research	https://doi.org/10.1029/2003JB002425	https://doi.org/10.17592/001.2021110904	-9999	Incoherent	168.7	VHF179	179
NIPR_2007_JARE49_GRN_BM3	Dome Fuji (JARE49)	Japanese Antarctic Research Expedition; National Institute of Polar Research	https://doi.org/10.5194/tc-6-1203-2012	https://doi.org/10.17592/001.2022072203 https://doi.org/10.17592/001.2022072204 https://doi.org/10.17592/001.2021110905 https://doi.org/10.17592/001.2021110906	-9999	Coherent; Incoherent	168.7	POL179; VHF60	179; 60
NIPR_2007_JASE_GRN_BM3	Dome Fuji (JASE)	Japanese Antarctic Research Expedition; National Institute of Polar Research; Stockholm University	https://doi.org/10.5194/tc-6-1203-2012	https://doi.org/10.17592/001.2022072205; https://doi.org/10.17592/001.2022072206; https://doi.org/10.17592/001.2022072207; https://doi.org/10.17592/001.2022072208; https://doi.org/10.17592/001.2022072209; https://doi.org/10.17592/001.2022072210; https://doi.org/10.17592/001.2022072211	-9999	Incoherent	168.7	VHF179	179
NIPR_2012_JARE54_GRN_BM3	Dome Fuji (JARE54)	Japanese Antarctic Research Expedition; National Institute of Polar Research	https://doi.org/10.5194/tc-16-2967-2022	https://doi.org/10.17592/001.2021110907	-9999	Coherent	168.7	POL179	179
NIPR_2017_JARE59_GRN_BM3	Dome Fuji (JARE59)	Japanese Antarctic Research Expedition; National Institute of Polar Research	https://doi.org/10.5194/tc-16-2967-2022	https://doi.org/10.17592/001.2021110908; https://doi.org/10.17592/001.2021110909	-9999	Coherent; Incoherent	168.7	POL179; VHF179	179

NIPR_2018_JARE60_GRN_BM3	Dome Fuji (JARE60)	Japanese Antarctic Research Expedition; National Institute of Polar Research	https://doi.org/10.5194/tc-16-2967-2022	http://doi.org/10.17592/001.2021110910	-9999	Incoherent	168.7	VHF179	179
KOPRI_2017_KRT1_AIR_BM3	David Glacier (KRT1)	Korea Polar Research Institute	https://doi.org/10.5194/tc-14-2217-2020	https://doi.org/10.5281/zenodo.3778452	0	2-D Synthetic Aperture Radar focusing	168.42	MARFA (UTIG)	60
KOPRI_2018_KRT2_AIR_BM3	David Glacier (KRT2)	Korea Polar Research Institute	https://doi.org/10.5194/tc-14-2217-2020	https://doi.org/10.5281/zenodo.3778452	0	2-D Synthetic Aperture Radar focusing	168.42	MARFA (UTIG)	60
NASA_2013_ICEBRIDGE_AIR_BM3	NASA Operation IceBridge	Center for Remote Sensing of Ice Sheets	https://doi.org/10.1029/2020RG000712	https://data.cresis.ku.edu/	0	2-D Synthetic Aperture Radar focused	169	MCoRDS V3	180-210
NASA_2014_ICEBRIDGE_AIR_BM3	NASA Operation IceBridge	Center for Remote Sensing of Ice Sheets	https://doi.org/10.1029/2020RG000712	https://data.cresis.ku.edu/	0	2-D Synthetic Aperture Radar focused	169	MCoRDS V2	165-215
NASA_2016_ICEBRIDGE_AIR_BM3	NASA Operation IceBridge	Center for Remote Sensing of Ice Sheets	https://doi.org/10.1029/2020RG000712	https://data.cresis.ku.edu/	0	2-D Synthetic Aperture Radar focused	169	MCoRDS V2	165-215
NASA_2017_ICEBRIDGE_AIR_BM3	NASA Operation IceBridge	Center for Remote Sensing of Ice Sheets	https://doi.org/10.1029/2020RG000712	https://data.cresis.ku.edu/	0	2-D Synthetic Aperture Radar focused	169	MCoRDS V3; MCoRDS v6	180-210; 150-450
NASA_2018_ICEBRIDGE_AIR_BM3	NASA Operation IceBridge	Center for Remote Sensing of Ice Sheets	https://doi.org/10.1029/2020RG000712	https://data.cresis.ku.edu/	0	2-D Synthetic Aperture Radar focused	169	MCoRDS V2	165-215
NASA_2019_ICEBRIDGE_AIR_BM3	NASA Operation IceBridge	Center for Remote Sensing of Ice Sheets	https://doi.org/10.1029/2020RG000712	https://data.cresis.ku.edu/	0	2-D Synthetic Aperture Radar focused	169	MCoRDS V7	236-254
NPI_2012_ICERISES_GRN_BM3	Dronning Maud Land ice rises	Norwegian Polar Institute	https://doi.org/10.5194/tc-11-2883-2017	https://doi.org/10.21334/npolar.2019.50edbcc2	5	Incoherent	169	NPI radar	2
NPI_2015_POLARGAP_AIR_BM3	Recovery Subglacial Lakes (PolarGAP)	Norwegian Polar Institute	https://doi.org/10.1029/2018JF004799	https://doi.org/10.21334/npolar.2019.ae99f750	10	2-D Synthetic Aperture Radar	168.5	PASIN (BAS)	150
NPI_2016_MADICE_GRN_BM3	Dronning Maud Land (MADICE)	Norwegian Polar Institute	https://doi.org/10.5194/tc-13-2579-2019	https://doi.org/10.21334/npolar.2020.9ca8826d	2	Incoherent	168	NPI radar	5
PRIC_2015_CHA1_AIR_BM3	Princess Elizabeth Land (CHA1)	Polar Research Institute of China	https://doi.org/10.5194/essd-12-2765-2020	https://doi.org/10.5281/zenodo.4023393	0	2-D Synthetic Aperture Radar focused	168	HiCARS (UTIG)	60
PRIC_2016_CHA2_AIR_BM3	Princess Elizabeth Land (CHA2)	Polar Research Institute of China	https://doi.org/10.5194/essd-12-2765-2020	https://doi.org/10.5281/zenodo.4023393	0	2-D Synthetic Aperture Radar focused	168	HiCARS (UTIG)	60

PRIC_2017_CHA3_AIR_BM3	Princess Elizabeth Land (CHA3)	Polar Research Institute of China	https://doi.org/10.5194/essd-12-2765-2020	https://doi.org/10.5281/zenodo.4023393	0	Coherent and incoherent stacking	168	HiCARS (UTIG)	60
PRIC_2018_CHA4_AIR_BM3	Princess Elizabeth Land (CHA4)	Polar Research Institute of China	https://doi.org/10.5194/essd-12-2765-2020	https://doi.org/10.5281/zenodo.4023393	0	Coherent and incoherent stacking	168	HiCARS (UTIG)	60
RNRF_1971_Lambert-Amery_SEI_BM3	Lambert Ice Shelf; Amery Ice Shelf	Polar Marine Geosurvey Expedition	https://doi.org/10.31857/S2076673421040110	-9999	-9999	-9999	-9999	seismic	-9999
RNRF_1975_Lazarev_SEI_BM3	Lazarev Ice Shelf	Polar Marine Geosurvey Expedition	https://doi.org/10.31857/S2076673421040110	-9999	-9999	-9999	-9999	seismic	-9999
RNRF_1975_Filchner-Ronne_SEI_BM3	Filchner Ronne Ice Shelf	Polar Marine Geosurvey Expedition	https://doi.org/10.31857/S2076673421040110	-9999	-9999	-9999	-9999	seismic	-9999
RNRF_2003_AMSap5_AIR_BM3	Princess Elizabeth Land	Polar Marine Geosurvey Expedition	https://doi.org/10.1017/aog.2020.4	-9999	0	Incoherent	168	MPI-60	60
RNRF_2004_AMSap5_AIR_BM3	Princess Elizabeth Land	Polar Marine Geosurvey Expedition	https://doi.org/10.1017/aog.2020.4	-9999	0	Incoherent	168	MPI-60	60
RNRF_2004_Mirny-Vostok_AIR_BM3	Mirny Station; Vostok Subglacial Lake	Polar Marine Geosurvey Expedition	https://doi.org/10.1017/aog.2020.4	-9999	0	Incoherent	168	MPI-60	60
RNRF_2005_AMSap5_AIR_BM3	Princess Elizabeth Land	Polar Marine Geosurvey Expedition	https://doi.org/10.1017/aog.2020.4	-9999	0	Incoherent	168	MPI-60	60
RNRF_2006_RAEap5_AIR_BM3	Princess Elizabeth Land	Polar Marine Geosurvey Expedition	https://doi.org/10.1017/aog.2020.4	-9999	0	Incoherent	168	MPI-60	60
RNRF_2006_Komsom-Vostok_AIR_BM3	Komsomolskaya Station; Vostok Subglacial Lake	Polar Marine Geosurvey Expedition	https://doi.org/10.1017/aog.2020.4	-9999	0	Incoherent	168	MPI-60	60
RNRF_2007_AMSap5_AIR_BM3	Princess Elizabeth Land	Polar Marine Geosurvey Expedition	https://doi.org/10.1017/aog.2020.4	-9999	0	Incoherent	168	MPI-60	60
RNRF_2008_AMSap5_AIR_BM3	Princess Elizabeth Land	Polar Marine Geosurvey Expedition	https://doi.org/10.1017/aog.2020.4	-9999	0	Incoherent	168	MPI-60	60
RNRF_2009_RAEap5_AIR_BM3	Princess Elizabeth Land	Polar Marine Geosurvey Expedition	https://doi.org/10.1017/aog.2020.4	-9999	0	Incoherent	168	MPI-60	60
RNRF_2010_RAE_AIR_BM3	Princess Elizabeth Land	Polar Marine Geosurvey Expedition	https://doi.org/10.1017/aog.2020.4	-9999	0	Incoherent	168	MPI-60	60
RNRF_2011_RAE_AIR_BM3	Princess Elizabeth Land	Polar Marine Geosurvey Expedition	https://doi.org/10.1017/aog.2020.4	-9999	0	Incoherent	168	MPI-60	60
RNRF_2013_RAE_AIR_BM3	Princess Elizabeth Land	Polar Marine Geosurvey Expedition	https://doi.org/10.1017/aog.2020.4	-9999	0	Incoherent	168	MPI-60	60
RNRF_2014_RAE_AIR_BM3	Princess Elizabeth Land	Polar Marine Geosurvey Expedition	https://doi.org/10.1017/aog.2020.4	-9999	0	Incoherent	168	MPI-60	60
RNRF_2015_RAE_AIR_BM3	Princess Elizabeth Land	Polar Marine Geosurvey Expedition	https://doi.org/10.1017/aog.2020.4	-9999	0	Incoherent	168	MPI-60	60

RNRF_2016_RAE_AIR_BM3	Princess Elizabeth Land	Polar Marine Geosurvey Expedition	https://doi.org/10.1017/aog.2020.4	-9999	0	Incoherent	168	MPI-60	60
RNRF_2017_RAE_AIR_BM3	Princess Elizabeth Land	Polar Marine Geosurvey Expedition	https://doi.org/10.1017/aog.2020.4	-9999	0	Incoherent	168	MPI-60	60
RNRF_2018_RAE_AIR_BM3	Princess Elizabeth Land	Polar Marine Geosurvey Expedition	https://doi.org/10.1017/aog.2020.4	-9999	0	Incoherent	168	MPI-60	60
RNRF_2019_RAE_AIR_BM3	Princess Elizabeth Land	Polar Marine Geosurvey Expedition	https://doi.org/10.1017/aog.2020.4	-9999	0	Incoherent	168	MPI-60	60
STANFORD_1971_SPRI-NSF-TUD_AIR_BM3	Antarctic-wide (SPRI-NSF-TUD surveys)	Stanford University	https://doi.org/10.1073/pnas.1821646116	https://doi.org/10.25740/ykq4-9345	-9999	-9999	168.5	SPRI/NSF/TUD radar	60; 300
ULB_2012_BEWISE_GRN_BM3	Dronning Maud Land ice rises (BeWise)	Université Libre de Bruxelles	https://doi.org/10.1017/jog.2016.7	https://doi.pangea.de/10.1594/PANGAEA.905997	6.5	Incoherent	168	NPI radar	10
ULB_2012_ICECON_GRN_BM3	Dronning Maud Land ice rises (IceCon)	Université Libre de Bruxelles	https://doi.org/10.1002/2014JF003246	https://doi.org/10.1594/PANGAEA.905315	8.8	Incoherent	168	NPI radar	2
UTIG_2009_Darwin-Hatherton_AIR_BM3	David and Hatherton glacier system	University of Texas Institute for Geophysics	http://doi.org/10.1017/jog.2017.60	https://doi.org/10.15784/601605	0	pik1 (short coherent)	168.4	HiCARS	60
UTIG_2010_ICECAP_AIR_BM3	Antarctic-wide (ICECAP)	University of Texas Institute for Geophysics	https://doi.org/10.1038/nature10114	https://doi.org/10.5067/W2KXX0MYNJ9G	0	pik1 (short coherent)	168.4	HiCARS	60
UTIG_2013_GIMBLE_AIR_BM3	Marie Byrd Land (GIMBLE)	University of Texas Institute for Geophysics	https://doi.org/10.1038/ngeo1992	https://doi.org/10.15784/601001	0	2-D Synthetic Aperture Radar focused	168.4	HiCARS	60
UTIG_2015_EAGLE_AIR_BM3	East Antarctic coastline (EAGLE)	University of Texas Institute for Geophysics	https://doi.org/10.1098/rsta.2014.0297	https://doi.org/10.26179/5bcfffdabcf92	0	pik1 (short coherent)	168.4	MARFA	60
UTIG_2016_OLDICE_AIR_BM3	Dome C	University of Texas Institute for Geophysics	https://doi.org/10.1098/rsta.2014.0297	https://doi.org/10.15784/601355	0	2-D Synthetic Aperture Radar focused	168.4	MARFA	60
UWASHINGTON_2018_South-Pole-Lake_GRN_BM3	South Pole	University of Washington	https://doi.org/10.1017/aog.2020.32	https://hdl.handle.net/1773/45293	-9999	2-D migration	169	University of Washington radar	3